



## Evaluation of column-averaged methane in models and TCCON with a focus on the stratosphere

Andreas Ostler<sup>1</sup>, Ralf Sussmann<sup>1</sup>, Prabir K. Patra<sup>2</sup>, Sander Houweling<sup>3,4</sup>, Marko De Bruine<sup>3</sup>, Gabriele P. Stiller<sup>5</sup>, Florian J. Haenel<sup>5</sup>, Johannes Plieninger<sup>5</sup>, Philippe Bousquet<sup>6,7</sup>, Yi Yin<sup>6,7</sup>, Marielle Saunois<sup>6,7</sup>, Kaley A. Walker<sup>8</sup>, Nicholas M. Deutscher<sup>9,10</sup>, David W. T. Griffith<sup>9</sup>, Thomas Blumenstock<sup>6</sup>, Frank Hase<sup>6</sup>, Thorsten Warneke<sup>10</sup>, Zhiting Wang<sup>10</sup>, Rigel Kivi<sup>11</sup>, and John Robinson<sup>12</sup>

<sup>1</sup>Karlsruhe Institute of Technology, IMK-IFU, 82467 Garmisch-Partenkirchen, Germany

<sup>2</sup>Research Institute for Global Change, JAMSTEC, Yokohama, 236-0001, Japan

<sup>3</sup>Institute for Marine and Atmospheric Research Utrecht, Utrecht University, 3584 CC Utrecht, the Netherlands

<sup>4</sup>SRON Netherlands Institute for Space Research, 3584 CA Utrecht, the Netherlands

<sup>5</sup>Karlsruhe Institute of Technology, IMK-ASF, 76021 Karlsruhe, Germany

<sup>6</sup>Laboratoire des Sciences du Climat et de l'Environnement, IPSL-LSCE, CEA-CNRS-UVSQ, UMR8212, 91191 Gif-sur-Yvette, France

<sup>7</sup>Université de Versailles Saint Quentin en Yvelines, 78000 Versailles, France

<sup>8</sup>Department of Physics, University of Toronto, Toronto, Ontario M5S 1A7, Canada

<sup>9</sup>School of Chemistry, University of Wollongong, Wollongong, NSW 2522, Australia

<sup>10</sup>Institute of Environmental Physics, University of Bremen, 28334 Bremen, Germany

<sup>11</sup>Finnish Meteorological Institute, Arctic Research Center, 99600 Sodankylä, Finland

<sup>12</sup>Department of Atmospheric Research, National Institute of Water and Atmospheric Research (NIWA) Ltd, Wellington 6021, New Zealand

Correspondence to: Ralf Sussmann (ralf.sussmann@kit.edu)

Received: 14 March 2016 – Published in Atmos. Meas. Tech. Discuss.: 11 May 2016

Revised: 12 September 2016 – Accepted: 15 September 2016 – Published: 28 September 2016

**Abstract.** The distribution of methane (CH<sub>4</sub>) in the stratosphere can be a major driver of spatial variability in the dry-air column-averaged CH<sub>4</sub> mixing ratio (XCH<sub>4</sub>), which is being measured increasingly for the assessment of CH<sub>4</sub> surface emissions. Chemistry-transport models (CTMs) therefore need to simulate the tropospheric and stratospheric fractional columns of XCH<sub>4</sub> accurately for estimating surface emissions from XCH<sub>4</sub>. Simulations from three CTMs are tested against XCH<sub>4</sub> observations from the Total Carbon Column Network (TCCON). We analyze how the model–TCCON agreement in XCH<sub>4</sub> depends on the model representation of stratospheric CH<sub>4</sub> distributions. Model equivalents of TCCON XCH<sub>4</sub> are computed with stratospheric CH<sub>4</sub> fields from both the model simulations and from satellite-based CH<sub>4</sub> distributions from MIPAS (Michelson Interferometer for Passive Atmospheric Sounding) and MIPAS CH<sub>4</sub> fields adjusted to ACE-FTS (Atmospheric Chemistry Ex-

periment Fourier Transform Spectrometer) observations. Using MIPAS-based stratospheric CH<sub>4</sub> fields in place of model simulations improves the model–TCCON XCH<sub>4</sub> agreement for all models. For the Atmospheric Chemistry Transport Model (ACTM) the average XCH<sub>4</sub> bias is significantly reduced from 38.1 to 13.7 ppb, whereas small improvements are found for the models TM5 (Transport Model, version 5; from 8.7 to 4.3 ppb) and LMDz (Laboratoire de Météorologie Dynamique model with zooming capability; from 6.8 to 4.3 ppb). Replacing model simulations with MIPAS stratospheric CH<sub>4</sub> fields adjusted to ACE-FTS reduces the average XCH<sub>4</sub> bias for ACTM (3.3 ppb), but increases the average XCH<sub>4</sub> bias for TM5 (10.8 ppb) and LMDz (20.0 ppb). These findings imply that model errors in simulating stratospheric CH<sub>4</sub> contribute to model biases. Current satellite instruments cannot definitively measure stratospheric CH<sub>4</sub> to sufficient accuracy to eliminate these biases. Applying transport diag-

nostics to the models indicates that model-to-model differences in the simulation of stratospheric transport, notably the age of stratospheric air, can largely explain the inter-model spread in stratospheric CH<sub>4</sub> and, hence, its contribution to XCH<sub>4</sub>. Therefore, it would be worthwhile to analyze how individual model components (e.g., physical parameterization, meteorological data sets, model horizontal/vertical resolution) impact the simulation of stratospheric CH<sub>4</sub> and XCH<sub>4</sub>.

## 1 Introduction

The column-averaged dry-air mixing ratio of methane (CH<sub>4</sub>), denoted as XCH<sub>4</sub>, is an integrated measure of CH<sub>4</sub> with contributions from the troposphere and the stratosphere. Observations of XCH<sub>4</sub> contain source/sink information on a global to regional scale. They are provided by the ground-based networks NDACC (Network for the Detection of Atmospheric Composition Change, <http://www.ndacc.org/>; Kurylo, 1991; for XCH<sub>4</sub> retrievals see, e.g., Sussmann et al., 2011, 2012, 2013) and TCCON (Total Carbon Column Observing Network, <http://www.tcon.caltech.edu/>; Wunch et al., 2011), and also by satellite-based observation platforms like SCIAMACHY (Scanning Imaging Absorption Spectrometer for Atmospheric Cartography; Burrows et al., 1995; Frankenberg et al., 2011) and GOSAT (Greenhouse Gases Observing Satellite; Kuze et al., 2009; Yokota et al., 2009). Satellite-inferred XCH<sub>4</sub> observations are increasingly used in atmospheric inverse modeling because of their beneficial spatiotemporal data coverage (Bergamaschi et al., 2013; Fraser et al., 2013, 2014; Monteil et al., 2013; Houweling et al., 2014; Wecht et al., 2014; Cressot et al., 2014; Alexe et al., 2015; Turner et al., 2015; Locatelli et al., 2015). Given the high accuracy of ground-based XCH<sub>4</sub> TCCON retrievals, these observations are typically used for the evaluation of both chemistry-transport model (CTM) simulations (Saito et al., 2012; Belikov et al., 2013; Monteil et al., 2013; Fraser et al., 2014; Alexe et al., 2015; Turner et al., 2015) and satellite-retrieved XCH<sub>4</sub> (Parker et al., 2011, 2015; Schepers et al., 2012; Dils et al., 2014; Houweling et al., 2014; Parker et al., 2015; Kulawik et al., 2016; Pandey et al., 2016; Inoue et al., 2016).

Because of the various influences on XCH<sub>4</sub>, however, the interpretation of residual XCH<sub>4</sub> differences with TCCON may be difficult. For example, a good agreement between XCH<sub>4</sub> simulations and observations may suggest that a CTM is able to represent atmospheric conditions in a realistic way. However, it could also be the case that systematic model and satellite data errors in the troposphere and the stratosphere compensate each other. For this reason, it is necessary to extend model validations with additional atmospheric CH<sub>4</sub> observations that are complementary to XCH<sub>4</sub> observations, like surface or airborne in situ measurements, or balloon-based vertical profiles (Karion et al., 2010). In the

context of a refined model comparison, it is also possible to separate ground-based XCH<sub>4</sub> observations into tropospheric and stratospheric partial columns (Washenfelder et al., 2003; Sepúlveda et al., 2012, 2014; Wang et al., 2014; Saad et al., 2014).

Model–measurement XCH<sub>4</sub> residuals are minimized by atmospheric inversions in order to constrain CH<sub>4</sub> emission fluxes. Inversion models are also able to make use of in situ measurements and XCH<sub>4</sub> observations at the same time in order to adjust prior emission fluxes. Nevertheless, such inverse models still have to deal with ill-defined XCH<sub>4</sub> biases, which, in contrast to well-quantified biases, can only be attributed to errors in the model or the observations with an ambiguous assignment (Houweling et al., 2014). Currently, there are various approaches to optimize bias correction functions within the inverse model or to construct bias corrections as ad hoc functions of latitude or air mass. Ad hoc bias corrections, like removing a latitudinal background pattern in XCH<sub>4</sub> model–observation differences, are common, even though they bear the risk of obscuring real signals from emissions on the Earth's surface. Given the fact that the stratospheric contribution relative to the CH<sub>4</sub> total column increases from ~5% at the tropics up to ~25% at midlatitudes and high latitudes, model errors in the representation of stratospheric CH<sub>4</sub> mixing ratios are expected to give rise to a latitudinal varying bias (Turner et al., 2015). Although it is known that CTMs differ by up to ~50% in the simulation of lower stratospheric CH<sub>4</sub> distributions (Patra et al., 2011), an atmospheric region with a steep methane gradient of ~−50 ppb km<sup>−1</sup>, the impact of model errors in stratospheric CH<sub>4</sub> on XCH<sub>4</sub> has not been rigorously quantified up to now. In this context, the goal of this study is to better understand the sensitivity of XCH<sub>4</sub> model–observation differences to the model representation of stratospheric CH<sub>4</sub>.

Our XCH<sub>4</sub> model–observation analysis is based on optimized model simulations from three well-established CTMs on the one side and accurate XCH<sub>4</sub> observations from TCCON on the other. The impact of model stratospheric CH<sub>4</sub> distributions on XCH<sub>4</sub> is estimated by replacing modeled stratospheric CH<sub>4</sub> fields with monthly mean CH<sub>4</sub> distributions observed by MIPAS (Michelson Interferometer for Passive Atmospheric Sounding) and by ACE-FTS (Atmospheric Chemistry Experiment Fourier Transform Spectrometer). In addition to this, we briefly evaluate the model characteristics of stratospheric transport in order to understand differences between simulated and observed CH<sub>4</sub> distributions. The paper has the following structure: After introducing the models (Sect. 2) and the observations (Sect. 3), we present both a direct model–TCCON comparison and a comparison with refined model data using satellite data products of stratospheric CH<sub>4</sub> in Sect. 4. The transport characteristics of the models are discussed in Sect. 5, followed by a summary and conclusions in Sect. 6.

**Table 1.** Overview of CTMs used for model–TCCON comparison.

Model name	Institution	Resolution		Output CH <sub>4</sub>	Mean age derived from	Reference
		Horizontal <sup>a</sup>	Vertical <sup>b</sup>			
ACTM	JAMSTEC	~ 2.8 × 2.8°	67σ	1-hourly, monthly	idealized transport tracer simulations	Patra et al. (2016)
TM5	SRON	~ 6 × 4°	25η	daily	SF <sub>6</sub> simulations	Pandey et al. (2016)
LMDz	LSCE	~ 3.75 × 1.875°	39η	monthly	SF <sub>6</sub> simulations	Locatelli et al. (2015)

<sup>a</sup> Longitude × latitude. <sup>b</sup> Vertical coordinates in sigma-pressure σ (pressure divided by surface pressure) and hybrid sigma-pressure η.

## 2 Model simulations

The focus of this study is the assessment of the impact of stratospheric CH<sub>4</sub> on XCH<sub>4</sub>. Therefore, we try to ensure that model simulations represent tropospheric CH<sub>4</sub> mixing ratios as well as possible. For this purpose, we use optimized CH<sub>4</sub> model simulations that have been constrained by surface observations. Our model analysis comprises simulations from three well-established CTMs that have already been part of the chemistry-transport model intercomparison experiment TransCom-CH<sub>4</sub> (Patra et al., 2011) and used in inverse modeling of CH<sub>4</sub> emissions. Furthermore, we use model simulations of stratospheric mean age for an evaluation of model transport characteristics in Sect. 5. Basic model features are given in Table 1.

### 2.1 ACTM

The Atmospheric Chemistry Transport Model (ACTM) model (Patra et al., 2009a) is an atmospheric general circulation model (AGCM)-based CTM from the Center for Climate System Research/National Institute for Environmental Studies/Frontier Research Center for Global Change (CCSR/NIES/FRCGC). Here, we use optimized ACTM simulations presented in Patra et al. (2016) as inversion case 2 (CH<sub>4</sub>ags). The ACTM horizontal resolution is ~ 2.8° × 2.8° (T42 spectral truncations) with 67 sigma-pressure vertical levels. The meteorological fields of ACTM are nudged with reanalysis data from the Japan Meteorological Agency, version JRA-25 (Onogi et al., 2007). ACTM uses an optimized OH field (Patra et al., 2014) based on a scaled version of the seasonally varying OH field from Spivakovsky et al. (2000). The concentration fields that are relevant for stratospheric CH<sub>4</sub> loss – OH, O(<sup>1</sup>D), and chlorine (Cl) radicals – are based on simulations by the ACTM’s stratospheric model run (Takigawa et al., 1999). ACTM mean age is derived from the simulation of an idealized transport tracer with uniform surface fluxes, linearly increasing trend, and no loss in the atmosphere (Patra et al., 2009b). The ACTM simulates the observed CH<sub>4</sub> interhemispheric gradient in the troposphere and individual in situ measurements generally within 10 ppb (Patra et al., 2016).

### 2.2 TM5

The global chemistry Tracer Model, version 5 (TM5) has been described in Krol et al. (2005) and used as an atmospheric inversion model for CH<sub>4</sub> emissions (Bergamaschi et al., 2005; Meirink et al., 2008; Houweling et al., 2014). Here, we use TM5 simulations of CH<sub>4</sub> optimized with surface measurements only (Pandey et al., 2016). TM5 is run with a horizontal resolution of 6° × 4° and a vertical grid of 25 layers. TM5 meteorology is driven by the reanalysis data set ERA-Interim (Dee et al., 2011) from the European Centre for Medium Range Weather Forecasts (ECMWF). The simulation of the chemical CH<sub>4</sub> sink uses OH fields from Spivakovsky et al. (2000), which have been scaled to match methyl chloroform measurements. In addition to that, stratospheric CH<sub>4</sub> loss via Cl and O(<sup>1</sup>D) radicals is simulated using their concentration fields based on the 2-D photochemical Max Planck Institute (MPI) model (Brühl and Crutzen, 1993). Known deficiencies in the TM5 simulation of interhemispheric mixing have been corrected by extending the model with a horizontal diffusion parameterization that is adjusted to match SF<sub>6</sub> simulations with SF<sub>6</sub> measurements (Monteil et al., 2013).

TM5 simulations of sulfur hexafluoride (SF<sub>6</sub>) were used to derive stratospheric mean age data. SF<sub>6</sub> mixing ratios are monotonically increasing with time, showing higher mixing ratios in the troposphere than in the stratosphere, given the transport time from SF<sub>6</sub> surface sources to higher altitudes. This implies that tropospheric and stratospheric SF<sub>6</sub> mixing ratios of equal size are separated from each other by a time lag, which is commonly defined as mean age of air. In order to derive mean age from SF<sub>6</sub> model simulations, the same tropospheric SF<sub>6</sub> reference time series was used as for the derivation of MIPAS mean age data (see Stiller et al., 2012)

### 2.3 LMDz

The LMDz (Laboratoire de Météorologie Dynamique model with zooming capability) is a general circulation model (Hourdin et al., 2006), which has been used to investigate the impact of transport model errors on inverted CH<sub>4</sub> emissions (Locatelli et al., 2013). Here, we use optimized LMDz simulations of CH<sub>4</sub>, recently presented as LMDz-SP constrained

by surface measurements from background sites (Locatelli et al., 2015). These model simulations are nudged with the ERA-Interim reanalysis data set for horizontal winds ( $u$ ,  $v$ ). LMDz has a horizontal resolution of  $3.75^\circ \times 1.875^\circ$ , and 39 hybrid sigma-pressure layers. The chemical destruction of  $\text{CH}_4$  by OH and  $\text{O}(^1\text{D})$  is based on prescribed concentration fields simulated by the chemistry–climate model LMDz-INCA (Szopa et al., 2013). No Cl-based  $\text{CH}_4$  destruction is prescribed in this version of the model. Besides  $\text{CH}_4$ , LMDz simulations of  $\text{SF}_6$  were used to derive mean age data similarly to the method used for TM5.

### 3 Intercomparison strategy and observations

#### 3.1 Intercomparison strategy

We want to quantify the dependence of the  $\text{XCH}_4$  model–observation agreement on the model representation of stratospheric  $\text{CH}_4$  mixing ratios. For this purpose, we apply original  $\text{CH}_4$  model fields and two corrected  $\text{CH}_4$  model fields, where we have replaced the modeled stratospheric  $\text{CH}_4$  by satellite data sets of stratospheric  $\text{CH}_4$  mixing ratios. The first satellite data set consists of MIPAS  $\text{CH}_4$  observations, whereas the second satellite data set contains MIPAS  $\text{CH}_4$  observations that are adjusted to ACE-FTS-observed  $\text{CH}_4$  levels. This allows us to represent an uncertainty range for the satellite-based model correction. Finally, our  $\text{XCH}_4$  model–observation comparison deals with a triplet of model  $\text{CH}_4$  fields for each CTM.

Using TCCON  $\text{XCH}_4$  observations as validation reference, we evaluate the impact of correcting the modeled stratospheric  $\text{CH}_4$  on  $\text{XCH}_4$ . Consequently, modeled vertical profiles of  $\text{CH}_4$  were extracted for each TCCON site and subsequently converted to  $\text{XCH}_4$  by accounting for the TCCON retrieval a priori and vertical sensitivity. This means that model  $\text{CH}_4$  profiles are adjusted to the actual surface pressure measured at the time of a single TCCON observation. In addition to that, model profiles are convolved with the daily TCCON retrieval a priori profiles of  $\text{CH}_4$ , which have been converted from wet air into dry air units by subtracting a daily water vapor profile provided by NCEP (National Centers for Environmental Prediction) and the averaging kernel depending on the actual solar zenith angle. Thereby, monthly mean  $\text{CH}_4$  profiles from LMDz also receive a daily component depending on the surface pressure, the TCCON a priori profiles and averaging kernels. The statistical analysis of  $\text{XCH}_4$  model–TCCON differences is then based on the daily mean time series for the year 2010.

#### 3.2 TCCON observations of column-averaged methane

Solar absorption measurements in the near-infrared are performed via ground-based Fourier transform spectrometers (FTSs) at TCCON sites across the globe. TCCON-type measurements are analyzed with the GGG software package, in-

cluding the spectral fitting code GFIT to derive total column abundances of several trace gases (Wunch et al., 2011). The  $\text{CH}_4$  total column is inverted from the spectra in three different spectral windows centered at 5938, 6002, and  $6076 \text{ cm}^{-1}$ . The spectral fitting method is based on iteratively scaling a priori profiles to provide the best fit to the measured spectrum. The general shape of the a priori profiles has been inferred from aircraft, balloon and satellite profiles (ACE-FTS profiles measured in the  $30\text{--}40^\circ \text{ N}$  latitude range from 2003 to 2007). In addition, the shape of the daily a priori profile is vertically squeezed/stretched depending on tropopause altitude and the latitude of the measurement site. This means that the tropopause altitude is used as a proxy for stratospheric ascent/descent to represent the origin of the air mass in the a priori profile.  $\text{XCH}_4$  is calculated by dividing the  $\text{CH}_4$  number density by the simultaneously measured  $\text{O}_2$  number density (a proxy for the dry-air pressure column).

These  $\text{XCH}_4$  retrievals are corrected a posteriori for known air-mass-dependent biases and calibrated to account for air-mass-independent biases, which can, among other errors, arise from spectroscopic uncertainties (Wunch et al., 2011). The air-mass-independent calibration factor, which is determined by comparisons with coincident airborne or balloon-borne in situ measurements over TCCON sites (Wunch et al., 2010; Messerschmidt et al., 2011; Geibel et al., 2012), allows for a calibration of TCCON  $\text{XCH}_4$  retrievals to in situ measurements on the WMO scale. Furthermore, the quality of the retrievals is continuously improved by correcting the influence of systematic instrumental changes over time. As a result of these improvements there are different versions of the GGG software package. In this study we use TCCON retrievals performed with version GGG2014 (for details see <https://tcon-wiki.caltech.edu/>). The TCCON measurement precision ( $2\sigma$ ) for  $\text{XCH}_4$  is  $< 0.3\%$  ( $< 5 \text{ ppb}$ ) for single measurements. For the year 2010,  $\text{XCH}_4$  observations are available from 11 TCCON sites, listed in Table 2. Knowing that TCCON  $\text{XCH}_4$  accuracy can be affected by a strong polar vortex (Ostler et al., 2014), we exclude high-latitude observations at Sodankylä within the early spring period (March, April, May) from the analysis. TCCON data were obtained from the TCCON Data Archive, hosted by the Carbon Dioxide Information Analysis Center (CDIAC: <http://cdiac.ornl.gov/>). The individual data sets of the TCCON sites used in this study are available from this database.

#### 3.3 Satellite-based data sets of stratospheric methane

In order to correct modeled stratospheric  $\text{CH}_4$  fields, we use satellite-borne MIPAS measurements covering the stratosphere. As a Fourier-Transform Infrared Spectrometer aboard the Environmental Satellite (Envisat), MIPAS detected atmospheric emission spectra in the mid-infrared region via limb sounding (Fischer et al., 2008). Profiles of various atmospheric trace gas concentrations are derived by the research processor developed by the Karlsruhe Institute of

**Table 2.** Overview of TCCON measurement sites used for the evaluation of chemical transport models. Abbreviations of the site names, information about geographical location, and number of measurement days in 2010 are provided.

TCCON site	Abbreviation	Altitude	Latitude	Longitude	Days	Reference
Sodankylä (Finland)	SOD	188 m	67.4° N	26.6° E	78	Kivi et al. (2014)
Białystok (Poland)	BIA	180 m	53.2° N	23.0° E	120	Deutscher et al. (2014)
Karlsruhe (Germany)	KAR	110 m	49.1° N	8.4° E	79	Hase et al. (2014)
Orléans (France)	ORL	130 m	48.0° N	2.1° E	91	Warneke et al. (2014)
Garmisch (Germany)	GAR	743 m	47.5° N	11.1° E	120	Sussmann et al. (2014)
Park Falls (USA)	PAR	440 m	46.0° N	90.3° W	155	Wennberg et al. (2014a)
Lamont (USA)	LAM	320 m	36.6° N	97.5° W	299	Wennberg et al. (2014b)
Izaña (Tenerife)	IZA	2370 m	28.3° N	16.5° W	50	Blumenstock et al. (2014)
Darwin (Australia)	DAR	30 m	12.4° S	130.9° E	64	Griffith et al. (2014a)
Wollongong (Australia)	WOL	30 m	34.4° S	150.9° E	142	Griffith et al. (2014b)
Lauder (New Zealand)	LAU	370 m	45.0° S	169.7° E	142	Sherlock et al. (2014a, b)

Technology, Institute of Meteorology and Climate Research (KIT IMK) and the Instituto de Astrofísica de Andalucía (CSIC) (von Clarmann et al., 2003). The MIPAS CH<sub>4</sub> data set comprises zonal monthly means with a horizontal grid resolution of 5° latitude. In the vertical, the resolution of the MIPAS CH<sub>4</sub> fields range from 2.5 to 7 km; see Plieninger et al. (2015) for more details. As an additional quality criterion, we only select MIPAS data points that are averaged over more than 300 profile measurements. As a result, our MIPAS CH<sub>4</sub> data set typically covers altitudes higher than ~10 km at midlatitudes and heights above ~15 km in the tropics. This implies that we do not use a thermal or chemical tropopause definition, but use the MIPAS data where they are available. Therefore, we cannot exclude that our MIPAS-based CH<sub>4</sub> fields contain some upper tropospheric MIPAS values; i.e., our definition of stratospheric CH<sub>4</sub> is not strict from a meteorological point of view.

The corrected model CH<sub>4</sub> profiles rely on original model CH<sub>4</sub> fields that are merged with MIPAS-based zonal CH<sub>4</sub> fields (monthly means) interpolated to the model grid. Merging original model CH<sub>4</sub> fields/profiles with zonal monthly means implies that we lose some spatial and temporal variability in the corrected model CH<sub>4</sub> fields. For example, vertical shifts of the tropopause can cause significant variations in XCH<sub>4</sub> of ~25 ppb even within a day (Ostler et al., 2014). As these XCH<sub>4</sub> changes can be positive but also negative (tropopause shifted upwards and downwards), we expect that dynamically induced XCH<sub>4</sub> variations should be negligible from a statistical point of view as used in this study. For our aim – investigating the overall impact of model stratospheric CH<sub>4</sub> fields on the quantity XCH<sub>4</sub> – a monthly mean representation of stratospheric CH<sub>4</sub> in the corrected model fields is sufficient.

In our study we use the strongly revised MIPAS CH<sub>4</sub> data product for the MIPAS reduced-resolution period from January 2005 to April 2012. This new data set (version V5R\_CH4\_224/V5R\_CH4\_225) was recently introduced by Plieninger et al. (2015) with an emphasis on retrieval charac-

teristics. Plieninger et al. (2015) showed that CH<sub>4</sub> mixing ratios are reduced in the lowermost stratosphere when using the new retrieval settings. This finding implies that the high bias of the older CH<sub>4</sub> data version in the lowermost stratosphere, which was determined by Laeng et al. (2015), has been partially alleviated. Nevertheless, a recent comparison study by Plieninger et al. (2016) suggests a remaining positive bias (100–200 ppb) relative to other satellite measurements such as ACE-FTS observations.

For this reason, a second satellite CH<sub>4</sub> data set was constructed by adjusting MIPAS stratospheric CH<sub>4</sub> mixing ratios to ACE-FTS (Boone et al., 2013) measurements of CH<sub>4</sub>. Given the sparse data coverage of ACE-FTS observations for the year 2010, we did not use ACE-FTS measurements directly. Instead, the MIPAS CH<sub>4</sub> fields were adjusted by offsets relative to ACE shown in Fig. 1, yielding the second satellite-based CH<sub>4</sub> data set abbreviated by MIPAS\_ACE. We used collocated pairs of CH<sub>4</sub> profiles from MIPAS and ACE-FTS to derive a CH<sub>4</sub> offset as a function of altitude and latitude for the year 2010. The collocation criteria are based on a maximum radius of 500 km and a maximum temporal deviation of 5 h, which is identical to Plieninger et al. (2016). Furthermore, the MIPAS averaging kernels were applied to ACE-FTS CH<sub>4</sub> profiles. ACE-FTS operates in solar occultation mode (Bernath et al., 2005) and also provides retrievals of several trace gases including CH<sub>4</sub>. Here, we use ACE-FTS data from a research version of the 3.5 retrieval described in Buzan et al. (2016).

Figure 1 shows the CH<sub>4</sub> offset functions computed as mean differences between MIPAS and ACE-FTS for 30° latitudinal bands. Figure 1 confirms the findings by Plieninger et al. (2016) that MIPAS is biased positive by ~150 ppb relative to ACE-FTS within the lowermost stratosphere. For higher altitudes (> 25 km), mean differences between MIPAS and ACE-FTS are larger for the tropical domain (up to 100 ppb) compared to higher latitudes (up to 50 ppb).

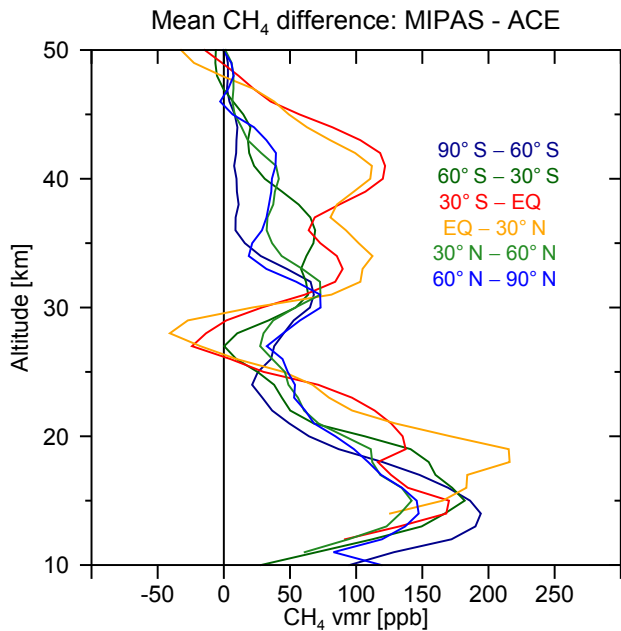


**Figure 1.** Mean  $\text{CH}_4$  differences between collocated MIPAS and ACE-FTS  $\text{CH}_4$  profiles measured in the year 2010. Mean  $\text{CH}_4$  differences in parts per billion (ppb) are derived for  $30^\circ$  latitudinal bands indicated by different colors.

### 3.4 MIPAS-observed mean age

Besides MIPAS  $\text{CH}_4$  observations, we also use MIPAS data sets of stratospheric mean age inferred from  $\text{SF}_6$  measurements. Here, we use the new MIPAS mean age data set presented by Haenel et al. (2015). This new mean age data set contains several improvements compared to the previous version introduced by Stiller et al. (2012). For MIPAS, the mean age is calculated as the average transport time from the tropical troposphere to a certain location in the stratosphere using NOAA (National Oceanic and Atmospheric Administration) observations as reference. The mean age of stratospheric air is of special interest for climate research because the distributions of greenhouse gases like ozone critically depend on possible changes in the stratospheric transport pathways (Engel et al., 2009). Mean age can be inferred from observations of clock tracers (concentrations monotonically increasing with time) like  $\text{SF}_6$  or  $\text{CO}_2$ , and can also be simulated by models. For this reason, it is a well-known diagnostic for stratospheric transport and is very suitable for the evaluation of model transport characteristics (Waugh and Hall, 2002). The combined MIPAS data set of stratospheric  $\text{CH}_4$  and mean age is used for the evaluation of model transport characteristics in Sect. 5.1.

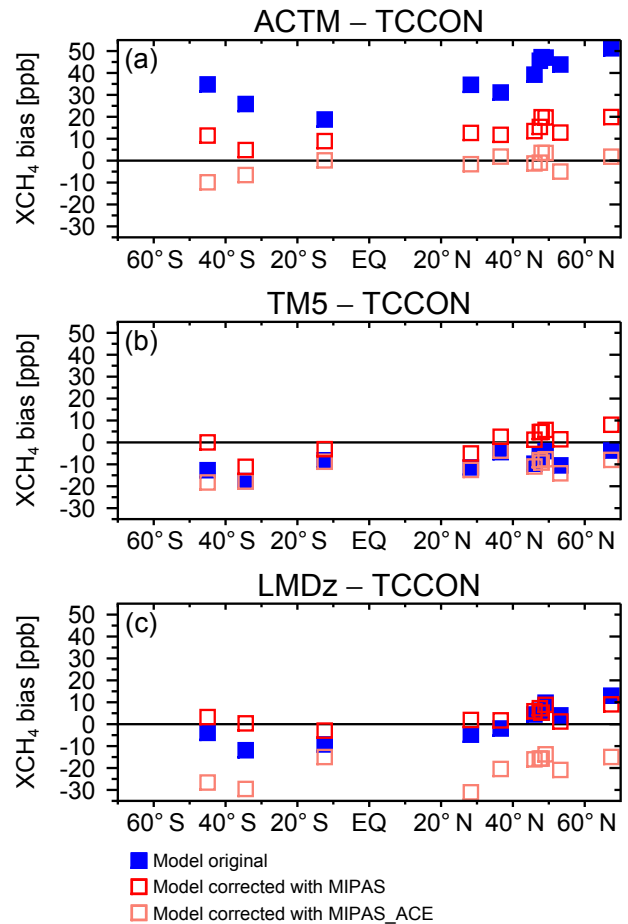


**Figure 2.** Site-specific model  $\text{XCH}_4$  biases with respect to TCCON observations in parts per billion (ppb) for the year 2010. Different colors indicate different stratospheric  $\text{CH}_4$  fields used for the calculation of model  $\text{XCH}_4$ .

## 4 Model–TCCON comparison of column-averaged methane

Figure 2 shows model biases in  $\text{XCH}_4$  with respect to TCCON observations, where each TCCON site is represented by its geographical latitude. For each CTM a triplet of model  $\text{CH}_4$  fields (uncorrected, MIPAS and MIPAS\_ACE corrected) yields a triplet of model  $\text{XCH}_4$  biases. All site-specific  $\text{XCH}_4$  model biases are individually listed in Table 3. In addition, Table 4 provides an average  $\text{XCH}_4$  bias for each model data set, computed as the mean of absolute site-specific biases.

The original  $\text{XCH}_4$  bias for ACTM lies between 18.8 and 51.3 ppb (see Fig. 2a and Table 3). This high bias is significantly reduced when ACTM stratospheric  $\text{CH}_4$  fields are replaced by satellite-based  $\text{CH}_4$  fields. The model correction with MIPAS  $\text{CH}_4$  reduces the average ACTM  $\text{XCH}_4$  bias from 38.1 to 13.7 ppb (see Table 4). Site-specific  $\text{XCH}_4$  biases are ranging from 4.8 to 19.9 ppb (see Table 3). The

**Table 3.** Site-specific model XCH<sub>4</sub> biases with respect to TCCON observations in 2010. The model–TCCON agreement in XCH<sub>4</sub> is evaluated with different stratospheric CH<sub>4</sub> model fields: the original model distribution (orig), the MIPAS-based stratospheric CH<sub>4</sub> (MIPAS), and the MIPAS-based stratospheric CH<sub>4</sub> adjusted to ACE-FTS observations (MIPAS\_ACE). XCH<sub>4</sub> biases and corresponding 2σ standard errors (in brackets) are in parts per billion (ppb).

Site	ACTM			TM5			LMDz		
	Orig	MIPAS	MIPAS_ACE	Orig	MIPAS	MIPAS_ACE	Orig	MIPAS	MIPAS_ACE
SOD	51.3 (±2.7)	19.9 (±2.9)	1.8 (±2.8)	−3.7 (±1.7)	8.1 (±2.6)	−8.0 (±2.5)	13.0 (±3.0)	9.1 (±3.2)	−15.0 (±3.6)
BIA	43.9 (±1.7)	12.8 (±1.7)	−5.0 (±1.9)	−10.5 (±1.3)	1.4 (±1.6)	−14.1 (±1.6)	4.0 (±1.7)	1.2 (±1.8)	−20.9 (±2.1)
KAR	47.0 (±2.0)	19.7 (±1.8)	3.5 (±1.9)	−4.0 (±1.4)	5.7 (±1.5)	−7.7 (±1.6)	9.8 (±2.0)	8.8 (±2.1)	−13.8 (±2.2)
ORL	47.2 (±1.7)	19.8 (±2.2)	3.5 (±2.3)	−7.0 (±1.5)	4.8 (±1.6)	−9.2 (±1.7)	5.4 (±2.1)	5.3 (±2.0)	−15.7 (±2.1)
GAR	45.6 (±1.8)	15.4 (±1.8)	−0.9 (±2.0)	−6.1 (±1.3)	4.7 (±1.5)	−8.1 (±1.5)	6.1 (±1.8)	7.3 (±1.8)	−15.7 (±1.8)
PAR	39.2 (±1.5)	13.5 (±1.6)	−1.3 (±1.6)	−9.7 (±1.2)	1.2 (±1.2)	−11.0 (±1.2)	4.4 (±1.4)	5.9 (±1.6)	−16.0 (±1.6)
LAM	31.1 (±1.3)	11.8 (±1.2)	1.8 (±1.1)	−4.4 (±0.8)	2.6 (±0.9)	−3.7 (±0.8)	−2.0 (±1.1)	1.7 (±1.1)	−20.4 (±1.2)
IZA	34.6 (±2.0)	12.6 (±2.2)	−1.6 (±2.2)	−11.4 (±1.5)	−5.0 (±1.5)	−12.6 (±1.5)	−4.8 (±1.9)	1.9 (±2.2)	−31.1 (±2.2)
DAR	18.8 (±1.6)	8.9 (±1.7)	0.1 (±1.8)	−8.1 (±1.0)	−3.1 (±1.1)	−8.8 (±1.1)	−9.2 (±1.6)	−2.9 (±2.6)	−15.0 (±1.4)
WOL	25.8 (±1.5)	4.8 (±1.6)	−6.6 (±1.6)	−17.6 (±1.4)	−11.1 (±1.4)	−17.9 (±1.3)	−11.9 (±1.8)	0.4 (±1.7)	−29.6 (±1.9)
LAU	34.8 (±1.0)	11.4 (±1.2)	−9.9 (±1.3)	−12.7 (±1.2)	0.0 (±1.3)	−18.3 (±1.3)	−4.0 (±1.4)	3.2 (±1.4)	−26.6 (±1.6)
Range	32.5	15.1	13.4	13.9	19.2	14.6	24.9	12.0	17.3

**Table 4.** Average model XCH<sub>4</sub> bias with respect to TCCON observations in 2010 computed as mean of absolute site-specific biases (see Table 3). Average XCH<sub>4</sub> biases in ppb are derived for different model stratospheric CH<sub>4</sub> fields.

Model stratospheric CH <sub>4</sub> field	Mean XCH <sub>4</sub> bias		
	ACTM	TM5	LMDz
Original model	38.1	8.7	6.8
MIPAS	13.7	4.3	4.3
MIPAS_ACE	3.3	10.8	20.0

model correction with MIPAS\_ACE reduces the average ACTM XCH<sub>4</sub> bias further from 38.1 to 3.3 ppb (see Table 4), with values in an interval between −9.9 and 3.5 ppb (see Table 3); values similar to that were expected from the comparison with ACTM simulations with tropospheric measurements (Patra et al., 2016).

For the original TM5 we detect negative site-specific XCH<sub>4</sub> biases with values between −17.6 and −3.7 ppb (see Fig. 2b and Table 3). When TM5 CH<sub>4</sub> fields are corrected with MIPAS observations, this negative XCH<sub>4</sub> bias is reduced from −8.7 to −4.3 ppb on average (see Table 3). The corresponding site-specific XCH<sub>4</sub> biases are then between −11.1 and 8.1 ppb (Table 3). If the MIPAS\_ACE is applied to TM5 then the site-specific TM5 XCH<sub>4</sub> biases are shifted further to the negative direction with values between −18.3 and −3.7 ppb. In this case the average XCH<sub>4</sub> bias increased from 8.7 to 10.8 ppb (Table 4).

With respect to TCCON observations LMDz produces both negative and positive XCH<sub>4</sub> biases ranging from −11.9 ppb (Wollongong) to 13.0 ppb (Sodankylä); see Fig. 2c and Table 3. The average LMDz XCH<sub>4</sub> bias is slightly reduced from 6.8 to 4.3 ppb if LMDz is corrected with MI-

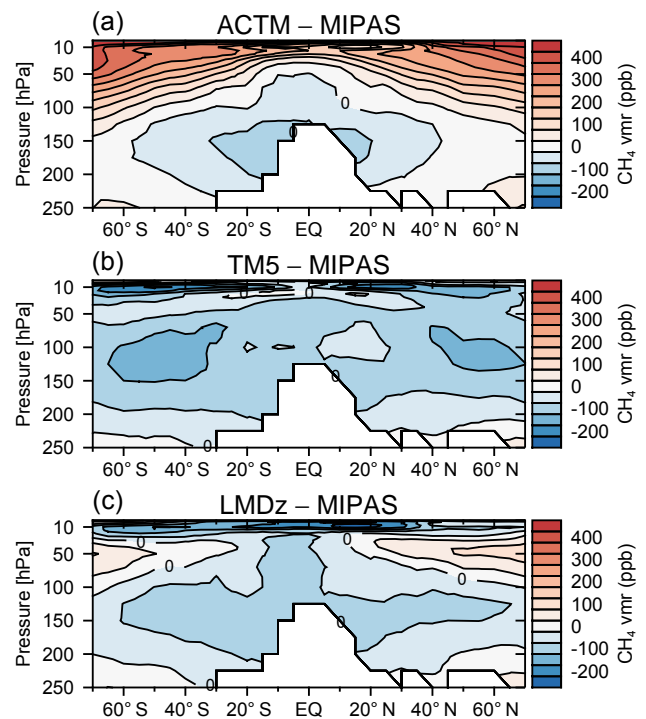


**Figure 3.** Model–MIPAS differences of stratospheric CH<sub>4</sub> volume mixing ratios (vmr) in parts per billion (ppb). Zonally averaged CH<sub>4</sub> vmr differences are annual means for the year 2010.

PAS CH<sub>4</sub> fields (see Table 4). After this correction, site-specific LMDz XCH<sub>4</sub> biases lie between −2.9 and 9.1 ppb. Using MIPAS\_ACE CH<sub>4</sub> fields for the LMDz model correction produces LMDz XCH<sub>4</sub> biases between −13.8 and −31.1 ppb. At the same time, the average LMDz XCH<sub>4</sub> bias is increased from 6.8 to 20.0 ppb (Table 4).

Overall, our results confirm that the model–TCCON agreement in  $XCH_4$  depends very much on the model representation of stratospheric  $CH_4$ . It is obvious that the  $XCH_4$  offset between ACTM and TCCON is significantly reduced with stratospheric  $CH_4$  fields based on satellite data. In contrast, for TM5 and LMDz, the impact of the model correction on the model–TCCON agreement is ambiguous, in that the model–TCCON agreement can be improved (with MIPAS), but can also be reduced (with MIPAS\_ACE). In order to understand this inter-model spread we look at the differences between modeled and satellite-retrieved  $CH_4$  fields. Figure 3 shows zonal and annual averaged  $CH_4$  mixing ratio differences between MIPAS and each CTM. Figure 3a illustrates that stratospheric  $CH_4$  mixing ratios are generally much higher in ACTM than in MIPAS. The ACTM–MIPAS differences in  $CH_4$  are increasing from negligible values within the lowermost stratosphere up to 450 ppb in the upper stratosphere. Furthermore, the ACTM–MIPAS difference in  $CH_4$  also shows a latitudinal dependence, with middle and upper stratospheric values increasing towards higher latitudes. The positive bias in stratospheric ACTM  $CH_4$  mixing ratios causes a positive ACTM bias in  $XCH_4$ . In contrast to that, we find negative model–MIPAS differences in stratospheric  $CH_4$  mixing ratios for TM5 (Fig. 3b), resulting in a small negative  $XCH_4$  bias. We identify two altitude regions, where TM5 modeled  $CH_4$  mixing ratios are smaller than MIPAS  $CH_4$  mixing ratios: the lower stratosphere with differences in  $CH_4$  mixing ratios of up to  $-100$  ppb, and the upper stratosphere ( $> 30$  hPa) with maximum  $CH_4$  differences of  $\sim -150$  ppb. Figure 3c shows the  $CH_4$  mixing ratio differences between LMDz and MIPAS with noticeable negative  $CH_4$  differences of up to  $-200$  ppb within the tropical upper stratosphere. Negative  $CH_4$  differences ( $\sim -100$  ppb) are also visible in the upper stratosphere of the midlatitude and high-latitude region. In contrast to this, we identify positive  $CH_4$  differences of up to 100 ppb within the middle stratosphere ( $\sim 50$  hPa) of the midlatitudes and high latitudes. The negative and positive  $CH_4$  differences partially cancel out in  $XCH_4$ . Similarly to Fig. 3, the  $CH_4$  differences between model and MIPAS\_ACE fields are illustrated in Fig. 4. Given the offset adjustment of MIPAS to ACE-FTS (see Fig. 1), the MIPAS\_ACE  $CH_4$  fields comprise lower  $CH_4$  mixing ratios compared to MIPAS, mostly in the lower stratosphere. Hence, the ACTM–satellite  $CH_4$  difference is larger for MIPAS\_ACE fields than for MIPAS fields. For TM5 and LMDz, model–satellite  $CH_4$  differences are shifted into the positive direction (Fig. 4b and c). In other words, modeled stratospheric  $CH_4$  mixing ratios appear to be too high when compared to MIPAS and too low in comparison to MIPAS\_ACE.

The zonal difference fields between model and satellite-based  $CH_4$  data sets have also been converted to  $XCH_4$  differences and are shown in Fig. 5. Two main features can be found in Fig. 5: (i) the  $XCH_4$  difference range between the two satellite-based data sets MIPAS (dark red) and MIPAS\_ACE (light red), which is  $\sim 27$  ppb ( $1\sigma$  standard deviation

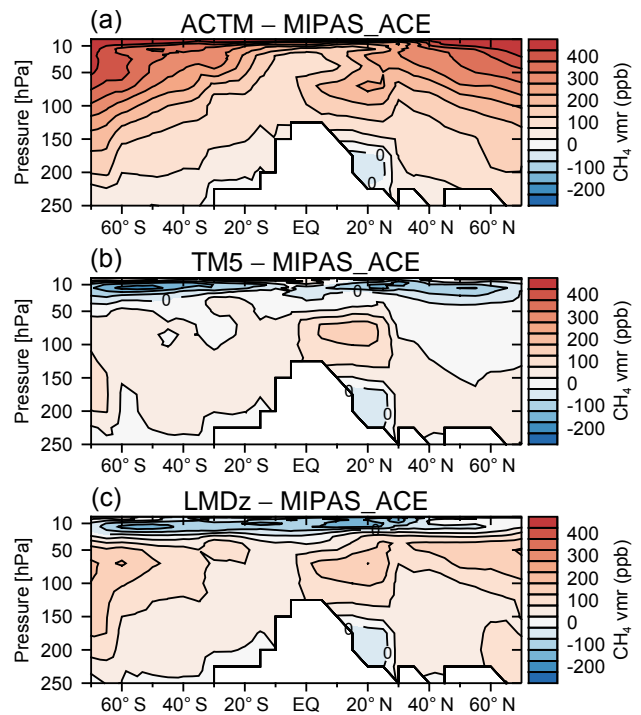


**Figure 4.** Model–MIPAS\_ACE differences of stratospheric  $CH_4$  volume mixing ratios (vmr) in parts per billion (ppb). Zonally averaged  $CH_4$  vmr differences are annual means for the year 2010.

tion (SD) = 4 ppb) on annual mean basis; and (ii) the model–satellite  $XCH_4$  differences, which indicate the latitudinal dependence of ACTM (Fig. 1a) and LMDz (Fig. 1c). For example, ACTM–satellite  $XCH_4$  differences are clearly increasing toward higher latitudes. In contrast to this, the TM5–satellite  $XCH_4$  difference does not show a latitudinal dependence. These findings on the latitudinal dependence of model–satellite  $XCH_4$  differences are supported by Table 5, which provides some statistical results. For example, the SDs and the minimum–maximum ranges of model–satellite  $XCH_4$  differences are much smaller for TM5 compared to the other models. Besides that, Fig. 5 also shows that the model–satellite  $XCH_4$  differences for the year 2010 only slightly depend on season. A noticeable seasonal variation in the model–satellite  $XCH_4$  differences can be found in the tropical/subtropical region of the Northern Hemisphere. However, in order to analyze seasonal variations, a more thorough analysis is needed, including model and satellite-based  $XCH_4$  data sets with a larger time period than used in this study. Furthermore, in the context of seasonality the role of TCCON station elevation needs to be considered in more detail. Since we only apply 1 year of model and satellite data, the focus of this study is not on the seasonal agreement between model and satellite-based  $XCH_4$  data sets.

Modeled stratospheric  $CH_4$  fields have been directly replaced by satellite data sets. As a result, there can be discontinuities in the merged  $CH_4$  fields around the tropopause,



**Table 5.** Average XCH<sub>4</sub> differences between model simulations and model CH<sub>4</sub> fields with satellite-based stratospheric CH<sub>4</sub> fields. Annual mean differences as XCH<sub>4</sub> bias (with 1σ SD) and minimum–maximum range of zonal XCH<sub>4</sub> differences are in ppb.

Satellite data	ACTM		TM5		LMDz	
	Bias	Min–max	Bias	Min–max	Bias	Min–max
MIPAS	22.3 (±14.1)	45.2	−13.9 (±3.4)	12.8	−4.3 (±9.4)	29.3
MIPAS_ACE	48.7 (±11.0)	35.4	13.6 (±3.5)	14.8	23.2 (±6.8)	22.3

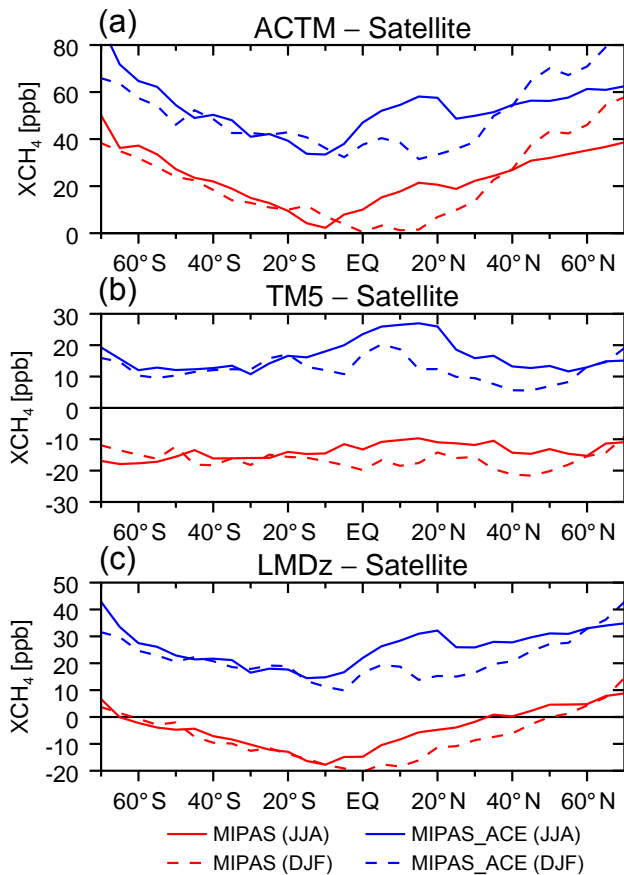


**Figure 5.** Zonal XCH<sub>4</sub> differences resulting from model–satellite differences of stratospheric CH<sub>4</sub> volume mixing ratios. Mean XCH<sub>4</sub> differences are shown as solid lines for the summer period (June, July, and August) and as dashed lines for the winter period (December, January, and February).

where the lowest satellite-based CH<sub>4</sub> mixing ratios strongly deviate from the original modeled CH<sub>4</sub> mixing ratios. In order to quantify the impact of these discontinuities on the XCH<sub>4</sub> data sets, we have also performed a smoother replacement method. For this purpose we defined a vertical transition range of 75 hPa, starting at the lowest vertical MIPAS data grid point. From this position the model vertical profile of CH<sub>4</sub> mixing ratios was linearly interpolated to the satellite-based CH<sub>4</sub> mixing ratio profile, starting at the upper boundary of this transition range. This method was applied

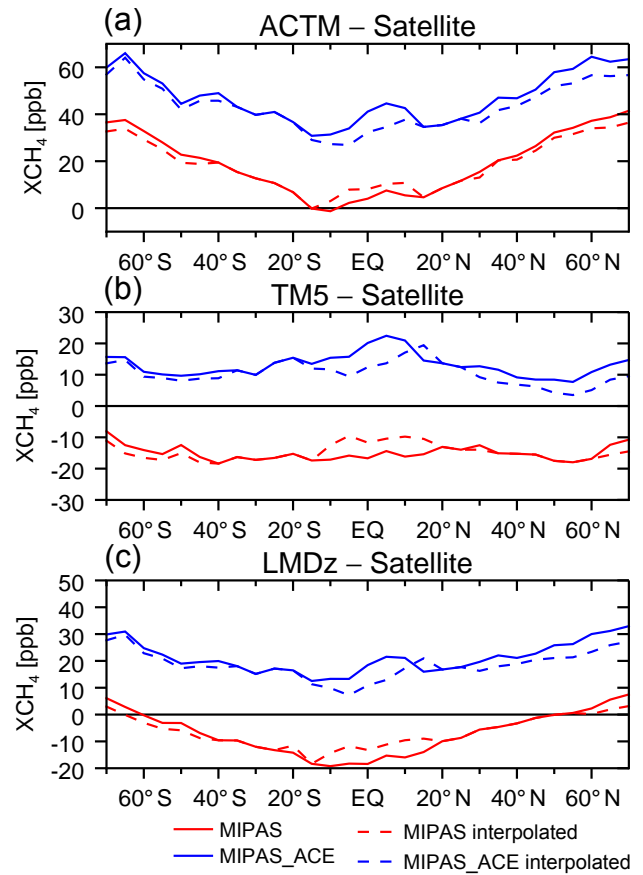


**Figure 6.** Zonal XCH<sub>4</sub> differences as a result of model–satellite differences of stratospheric CH<sub>4</sub> volume mixing ratios. Solid lines refer to the merged model–satellite CH<sub>4</sub> fields, including discontinuities at the model–satellite transition zone around the tropopause. Dashed lines refer to merged model–satellite CH<sub>4</sub> fields that have been smoothly interpolated at the model–satellite transition zone.

to each latitudinal MIPAS grid point corresponding to a vertical profile of CH<sub>4</sub> mixing ratios. The method was not used if the model–satellite difference of CH<sub>4</sub> mixing ratios was smaller than 30 ppb at the lower boundary of the transition range. Consequently, we also computed XCH<sub>4</sub> differences between the original model and the smoothed satellite-based data sets. Figure 6 then shows model–satellite XCH<sub>4</sub> differences resulting from the force replacement (solid lines) and from the smoothly interpolated replacement (dashed lines).

From Fig. 6 it is obvious that the impact of the smoothly interpolated replacement on the model–satellite  $XCH_4$  differences is small; i.e., differences between solid and dashed lines are typically smaller than 4 ppb. For this reason we expect that the impact of discontinuities in the merged model–satellite  $CH_4$  fields on the results of the  $XCH_4$  validation against TCCON is negligible.

## 5 Discussion

Our analysis shows that the model–TCCON agreement in  $XCH_4$  critically depends on the model representation of stratospheric  $CH_4$ , which is diverse for the presented CTMs. In the following we discuss possible causes for the inter-model spread in stratospheric  $CH_4$ . In addition to that, we evaluate the findings of our  $XCH_4$  model–TCCON comparison with respect to satellite data uncertainty.

### 5.1 Model transport characteristics as possible cause for inter-model spread in stratospheric methane

An inter-model spread in stratospheric  $CH_4$  fields has already been detected by Patra et al. (2011) despite applying uniform fields of OH, Cl, and  $O^1D$  for all models. Their findings, therefore, suggested a predominant role of transport in the simulation of  $CH_4$  vertical distributions. For this reason, here we tested whether differences in the modeling of stratospheric transport are noticeable. To do this, we follow the approach of Strahan et al. (2011) who sought to understand chemistry–climate model ozone simulations using transport diagnostics. This method is based on the compact relationship between a long-lived stratospheric tracer and mean age in the lower stratosphere. In their work, they compared simulations and air-borne observations of  $N_2O$ /mean age correlations, in order to evaluate the model transport characteristics. Here, we use the MIPAS data of  $CH_4$  and mean age as a reference to identify model-to-model differences in the simulation of stratospheric transport. The MIPAS data are not used to evaluate whether modeled stratospheric circulations are realistic or not, given the uncertainties of MIPAS  $CH_4$  and mean age data. For example, the MIPAS mean age range may be too large because MIPAS mean age can be up to 0.8 years too old due to the impact of mesospheric  $SF_6$  loss (Stiller et al., 2012). This loss process was not included in the models used for this study. Moreover, the MIPAS  $CH_4$  data significantly differ from ACE-FTS  $CH_4$  data within the lower stratosphere (see Fig. 1).

In analogy to Strahan et al. (2011) the model transport diagnostics are focused on the tropical domain because tropical diagnostics quantities allow a better assessment of the individual transport processes' ascent and mixing. Annual means of age for modeled as well as MIPAS-observed fields were calculated for the lower stratosphere (30–100 hPa) of the tropical domain ( $10^\circ S$ – $10^\circ N$ ), and of the northern hemi-

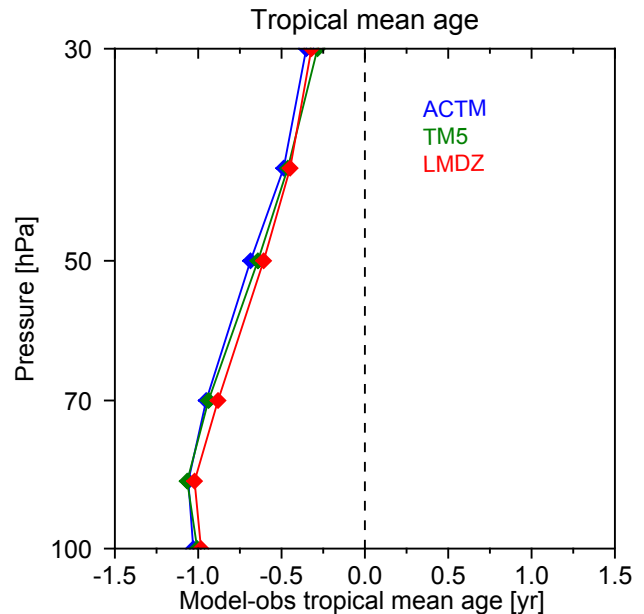


**Figure 7.** Model–MIPAS differences of mean age for the tropical lower. Mean age data in years (yr) are calculated as annual means on the MIPAS pressure–latitude grid.

spheric midlatitude region ( $35$ – $50^\circ N$ ), respectively. Subsequently, vertical profiles of mean model–MIPAS differences were calculated to provide insight into the tropical transport characteristics. Figure 7 illustrates that the model–MIPAS difference of tropical mean age is almost identical for all models; i.e. the model simulations produce similar mean ages that are younger than MIPAS-observed mean ages. Knowing that mean age represents the combined effects of ascent and mixing, we separately look at the tropical ascent rate, which is assessed by the horizontal mean age gradient, calculated as the difference between midlatitude and tropical mean ages. The model–MIPAS difference of the tropical ascent rate is shown in Fig. 8, indicating that ACTM and LMDz simulate tropical ascent in a similar way. The TM5-modeled tropical ascent is faster compared to ACTM and LMDz. Finally, these model transport diagnostics indicate model-to-model differences in the simulation of tropical ascent, which are likely to cause an inter-model spread in model stratospheric  $CH_4$  fields.

Indeed, model-to-model differences affecting the simulation of stratospheric transport are present in the vertical/horizontal resolution, sub-grid-scale physical parameterizations, advection schemes, and numerical methods, etc. Furthermore, the simulation of stratospheric transport depends on the reanalysis data used to drive the model meteorology; e.g., the ECMWF reanalysis data set ERA-Interim leads to an improved representation of the stratospheric circulation in comparison to the older ERA-40 reanalysis data (Mongee-Sanz et al., 2007, 2013; Diallo et al., 2012). The ERA-Interim data are used by TM5 and LMDz, whereas ACTM applies

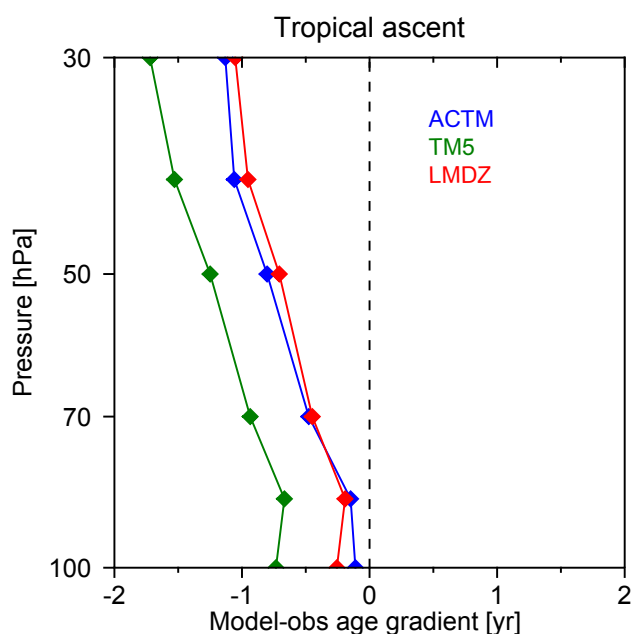


**Figure 8.** Model–MIPAS differences of the mean age gradient as a transport diagnostics for tropical ascent. The mean age gradient was calculated as the difference between the lower stratospheric mean ages averaged over 35–50° N and 10° S–10° N. Mean age data in years (yr) are calculated as annual means on the MIPAS pressure–latitude grid.

the JRA-25 reanalysis data (Onogi et al., 2007), which are known to have several deficiencies compared to the newer JRA-55 data (Ebita et al., 2011). However, testing ACTM with both ERA-Interim/40 and JRA-25/55 has not produced significant differences in CH<sub>4</sub> simulations (P. Patra, personal communication, 2016). Besides that, we do not expect that the poor representation of stratospheric CH<sub>4</sub> by ACTM (with 67 vertical levels) is impacted by a coarse vertical model grid resolution, as seen for an older version of LMDz (Locatelli et al., 2015).

## 5.2 Significance of satellite data range

The model correction with satellite-based CH<sub>4</sub> fields has an impact on the XCH<sub>4</sub> model–TCCON agreement, but the significance of this impact is diverse for the models. For ACTM, both satellite-based CH<sub>4</sub> fields, in particular MIPAS\_ACE, clearly yield an improved model–TCCON agreement. For TM5 and LMDz, the model–TCCON agreement can be slightly improved (with MIPAS), but also reduced (with MIPAS\_ACE). Thereby, we assert that original XCH<sub>4</sub> simulations from TM5 and LMDz lie inside the range that is spanned by the two satellite-based CH<sub>4</sub> fields. The most prominent feature of the satellite data range lies within the lower stratosphere where MIPAS-retrieved CH<sub>4</sub> mixing ratios are up to 200 ppb higher than ACE-FTS-retrieved CH<sub>4</sub> mixing ratios. Plieninger et al. (2016) also

found a similar high bias for MIPAS CH<sub>4</sub> data in comparison to satellite-based CH<sub>4</sub> observations from SCIAMACHY or HALOE (HALOgen Occultation Experiment). Furthermore, they showed that surface measurements provide CH<sub>4</sub> mixing ratios with slightly lower values than MIPAS-retrieved CH<sub>4</sub> mixing ratios of the upper troposphere, a finding that is against expectation. For these reasons, it is likely that our satellite data range is dominated by high biased lower stratospheric MIPAS CH<sub>4</sub> data. Thus, the model correction with ACE-FTS-based CH<sub>4</sub> fields seems more reliable. However, a definite assessment of the satellite data accuracies is not possible yet due to the lack of an extensive observational data set based on stratospheric in situ measurements.

## 6 Summary and conclusions

This study analyzed the importance of uncertainties in stratospheric CH<sub>4</sub> in comparisons of modeled and TCCON observed XCH<sub>4</sub>. Modeled stratospheric CH<sub>4</sub> fields were substituted by satellite-retrieved CH<sub>4</sub> fields from MIPAS and ACE-FTS. Original and satellite-corrected model CH<sub>4</sub> fields were converted to XCH<sub>4</sub> and subsequently evaluated by comparison to TCCON XCH<sub>4</sub> observations from 11 sites. This approach and the statistical analysis of XCH<sub>4</sub> model–TCCON residuals were conducted with three well-established CTMs: ACTM, TM5 and LMDz.

Our model–TCCON XCH<sub>4</sub> intercomparison reveals an inter-model spread in XCH<sub>4</sub> bias caused by an inter-model spread in stratospheric CH<sub>4</sub>. For ACTM we find a large average XCH<sub>4</sub> bias of 38.1 ppb, in contrast to small average XCH<sub>4</sub> biases of 8.7 ppb for TM5 and 6.8 ppb for LMDz. The ACTM XCH<sub>4</sub> bias is reduced by the model correction to 13.7 ppb with MIPAS, and to 3.3 ppb with MIPAS adjusted to ACE-FTS, respectively. For TM5 and LMDz the impact of the model correction with satellite-based CH<sub>4</sub> fields is ambiguous, in that the model XCH<sub>4</sub> bias can be slightly reduced to 4.3 ppb with MIPAS, but can also be increased to 10.8 ppb for TM5 and 20.0 ppb for LMDz with MIPAS adjusted to ACE-FTS. This implies that for TM5 and LMDz the model representation of stratospheric CH<sub>4</sub> is located within the satellite data range mapped by MIPAS and ACE-FTS observations. The annual mean differences between the two satellite-based stratospheric CH<sub>4</sub> fields yield a global XCH<sub>4</sub> difference range of ~ 27 ppb.

Possible causes for the inter-model spread in stratospheric CH<sub>4</sub> have been discussed with an emphasis on model transport characteristics. Applying tropical transport diagnostics suggests that the poor representation of stratospheric CH<sub>4</sub> by ACTM originates from errors in the simulation of transport pathways into and within the stratosphere. However, this is only an interpretation based on a diagnostic and requires more process-oriented model evaluation of stratospheric transport. The inter-model spread in stratospheric CH<sub>4</sub> could be quantitatively investigated with a main focus

on model-to-model differences in the simulation of stratospheric transport (physical parameterizations, reanalysis data sets, vertical/horizontal resolution); e.g., model simulations could be performed with different reanalysis data sets, and/or different physical parameterizations, resulting in a model ensemble for each CTM or a multi-model ensemble consisting of multiple CTM data sets. This would allow the individual model errors in stratospheric CH<sub>4</sub> to be assessed more precisely.

Overall we state that there is a need for improvement in modeling of stratospheric CH<sub>4</sub> and, thus, XCH<sub>4</sub>. At the same time, a better quantification of model errors in stratospheric CH<sub>4</sub> is limited by the uncertainty of satellite data products as used in this study. This implies that more stratospheric CH<sub>4</sub> in situ observations are required to validate both satellite-retrieved and modeled CH<sub>4</sub> data. A more accurate evaluation of modeled stratospheric CH<sub>4</sub> fields is particularly reasonable as these CTMs are used to invert CH<sub>4</sub> emissions from XCH<sub>4</sub> data. As surface emission signals in XCH<sub>4</sub> are small compared to co-resident XCH<sub>4</sub> atmospheric background levels, it is necessary to identify minor XCH<sub>4</sub> biases in the model as done in this study. Of course, an analogous quality requirement is also needed for ground-based and satellite-borne XCH<sub>4</sub> data. Indeed, as long as unallocated and poorly understood differences of several parts per billion remain between satellite-borne XCH<sub>4</sub> data and optimized model fields, it is difficult to make full benefit of satellite XCH<sub>4</sub> data to robustly retrieve regional methane emissions.

## 7 Data availability

TCCON data are publicly available at <http://www.tcon.caltech.edu/>; please follow the data use policy described there. For obtaining the model data used in this work, contact Prabir Patra ([prabir@jamstec.go.jp](mailto:prabir@jamstec.go.jp)) for ACTM, Sander Houweling ([S.Houweling@uu.nl](mailto:S.Houweling@uu.nl)) for TM5, and Philippe Bousquet ([philippe.bousquet@lsce.ipsl.fr](mailto:philippe.bousquet@lsce.ipsl.fr)) for LMDz. MIPAS and ACE satellite data are available from the official websites after signing a data protocol.

**Acknowledgements.** We thank H. P. Schmid (KIT/IMK-IFU) for his continual interest in this work. Our work has been performed as part of the ESA GHG-cci project via subcontract with the University of Bremen. In addition we acknowledge funding by the EC within the InGOS project. A part of work at JAXA was supported by the Environment Research and Technology Development Fund (A-1102) of the Ministry of the Environment, Japan. From 2004 to 2011 the Lauder TCCON program was funded by the New Zealand Foundation of Research Science and Technology contracts CO1X0204, CO1X0703 and CO1X0406. Since 2011 the program has been funded by NIWA's Atmosphere Research Program 3 (2011/13 Statement of Corporate Intent). The Darwin and Wollongong TCCON sites are funded by NASA grants NAG5-12247 and NNG05-GD07G, and Australian Research Council grants DP140101552, DP110103118, DP0879468, LE0668470, and LP0562346. We are

grateful to the DOE ARM program for technical support at the Darwin TCCON site. The Białystok and Orléans TCCON sites are funded by the EU projects InGOS and ICOS-INWIRE, and by the Senate of Bremen. Nicholas Deutscher was supported by an Australian Research Council fellowship, DE140100178. We are also grateful to P. O. Wennberg for providing TCCON data.

The Atmospheric Chemistry Experiment (ACE), also known as SCISAT, is a Canadian-led mission mainly supported by the Canadian Space Agency and the Natural Sciences and Engineering Research Council of Canada.

The article processing charges for this open-access publication were covered by a Research Centre of the Helmholtz Association.

Edited by: H. Worden

Reviewed by: C. Frankenberg and one anonymous referee

## References

- Alexe, M., Bergamaschi, P., Segers, A., Detmers, R., Butz, A., Hasekamp, O., Guerlet, S., Parker, R., Boesch, H., Frankenberg, C., Scheepmaker, R. A., Dlugokencky, E., Sweeney, C., Wofsy, S. C., and Kort, E. A.: Inverse modelling of CH<sub>4</sub> emissions for 2010–2011 using different satellite retrieval products from GOSAT and SCIAMACHY, *Atmos. Chem. Phys.*, 15, 113–133, doi:10.5194/acp-15-113-2015, 2015.
- Belikov, D. A., Maksyutov, S., Sherlock, V., Aoki, S., Deutscher, N. M., Dohe, S., Griffith, D., Kyro, E., Morino, I., Nakazawa, T., Notholt, J., Rettinger, M., Schneider, M., Sussmann, R., Toon, G. C., Wennberg, P. O., and Wunch, D.: Simulations of column-averaged CO<sub>2</sub> and CH<sub>4</sub> using the NIES TM with a hybrid sigma-isentropic ( $\sigma$ - $\theta$ ) vertical coordinate, *Atmos. Chem. Phys.*, 13, 1713–1732, doi:10.5194/acp-13-1713-2013, 2013.
- Bergamaschi, P., Krol, M., Dentener, F., Vermeulen, A., Meinhardt, F., Gaul, R., Ramonet, M., Peters, W., and Dlugokencky, E. J.: Inverse modelling of national and European CH<sub>4</sub> emissions using the atmospheric zoom model TM5, *Atmos. Chem. Phys.*, 5, 2431–2460, doi:10.5194/acp-5-2431-2005, 2005.
- Bergamaschi, P., Houweling, S., Segers, A., Krol, M., Frankenberg, C., Scheepmaker, R. A., Dlugokencky, E., Wofsy, S. C., Kort, E. A., Sweeney, C., Schuck, T., Brenninkmeijer, C., Chen, H., Beck, V., and Gerbig, C.: Atmospheric CH<sub>4</sub> in the first decade of the 21st century: inverse modeling analysis using SCIAMACHY satellite retrievals and NOAA surface measurements, *J. Geophys. Res.*, 118, 7350–7369, doi:10.1002/jgrd.50480, 2013.
- Bernath, P. F., McElroy, C. T., Abrams, M. C., Boone, C. D., Butler, M., Camy-Peyret, C., Carleer, M., Clerbaux, C., Coheur, P., Colin, R., DeCola, P., De Mazière, M., Drummond, J. R., Dufour, D., Evans, W. F. J., Fast, H., Fussen, D., Gilbert, K., Jennings, D. E., Llewellyn, E. J., Lowe, R. P., Mahieu, E., McConnell, J. C., McHugh, M., McLeod, S. D., Michaud, R., Midwinter, C., Nassar, R., Nichitui, F., Nowlan, C., Rinsland, C. P., Rochon, Y. J., Rowlands, N., Semeniuk, K., Simon, P., Skelton, R., Sloan, J. J., Soucy, M., Strong, K., Tremblay, P., Turnbull, D., Walker, K. A., Walkty, I., Wardle, D. A., Wehrle, V., Zander, R., and Zou, J.: Atmospheric Chemistry Experiment (ACE): Mission overview,

- Geophys. Res. Lett., 32, L15S01, doi:10.1029/2005GL022386, 2005.
- Blumenstock, T., Hase, F., Schneider, M., García, O. E., and Sepúlveda, E.: TCCON data from Izana, Tenerife, Spain, release GGG2014R0, TCCON data archive, hosted by the Carbon Dioxide Information Analysis Center, Oak Ridge National Laboratory, Oak Ridge, Tennessee, USA, doi:10.14291/tcon.ggg2014.izana01.R0/1149295, 2014.
- Boone, C. D., Walker, K. A., and Bernath, P. F.: Version 3 Retrievals for the Atmospheric Chemistry Experiment Fourier Transform Spectrometer (ACE-FTS), in: The Atmospheric Chemistry Experiment ACE at 10: A Solar Occultation Anthology, edited by: Bernath, P. F., A. Deepak Publishing, Hampton, Virginia, USA, 103–127, 2013.
- Brühl, C. and Crutzen, P. J.: The MPIC 2D model, in: NASA Ref. Publ. 1292, 1, 103–104, 1993.
- Burrows, J. P., Hölzle, E., Goede, A. P. H., Visser, H., and Fricke, W.: SCIAMACHY – Scanning Imaging Absorption Spectrometer for Atmospheric Cartography, *Acta Astronautica*, 35, 445–451, 1995.
- Cressot, C., Chevallier, F., Bousquet, P., Crevoisier, C., Dlugokencky, E. J., Fortems-Cheiney, A., Frankenberg, C., Parker, R., Pison, I., Scheepmaker, R. A., Montzka, S. A., Krummel, P. B., Steele, L. P., and Langenfelds, R. L.: On the consistency between global and regional methane emissions inferred from SCIAMACHY, TANSO-FTS, IASI and surface measurements, *Atmos. Chem. Phys.*, 14, 577–592, doi:10.5194/acp-14-577-2014, 2014.
- Buzan, E. M., Beale, C. A., Boone, C. D., and Bernath, P. F.: Global stratospheric measurements of the isotopologues of methane from the Atmospheric Chemistry Experiment Fourier transform spectrometer, *Atmos. Meas. Tech.*, 9, 1095–1111, doi:10.5194/amt-9-1095-2016, 2016.
- Dee, D. P., Uppala, S. M., Simmons, A. J., Berrisford, P., Poli, P., Kobayashi, S., Andrae, U., Balmaseda, M. A., Balsamo, G., Bauer, P., Bechtold, P., Beljaars, A. C. M., van de Berg, L., Bidlot, J., Bormann, N., Delsol, C., Dragani, R., Fuentes, M., Geer, A. J., Haimberger, L., Healy, S. B., Hersbach, H., Hólm, E. V., Isaksen, I., Kållberg, P., Köhler, M., Matricardi, M., McNally, A. P., Monge-Sanz, B. M., Morcrette, J.-J., Park, B.-K., Peubey, C., de Rosnay, P., Tavolato, C., Thépaut, J.-N., and Vitart, F.: The ERA-Interim reanalysis: configuration and performance of the data assimilation system, *Q. J. Roy. Meteor. Soc.*, 137, 553–597, doi:10.1002/qj.828, 2011.
- Deutscher, N., Notholt, J., Messerschmidt, J., Weinzierl, C., Warneke, T., Petri, C., Gruppe, P., and Katrynski, K.: TCCON data from Bialystok, Poland, Release GGG2014R0, TCCON data archive, hosted by the Carbon Dioxide Information Analysis Center, Oak Ridge National Laboratory, Oak Ridge, Tennessee, USA, doi:10.14291/tcon.ggg2014.bialystok01.R0/1149277, 2014.
- Diallo, M., Legras, B., and Chédin, A.: Age of stratospheric air in the ERA-Interim, *Atmos. Chem. Phys.*, 12, 12133–12154, doi:10.5194/acp-12-12133-2012, 2012.
- Dils, B., Buchwitz, M., Reuter, M., Schneising, O., Boesch, H., Parker, R., Guerlet, S., Aben, I., Blumenstock, T., Burrows, J. P., Butz, A., Deutscher, N. M., Frankenberg, C., Hase, F., Hasekamp, O. P., Heymann, J., De Mazière, M., Notholt, J., Sussmann, R., Warneke, T., Griffith, D., Sherlock, V., and Wunch, D.: The Greenhouse Gas Climate Change Initiative (GHG-CCI): comparative validation of GHG-CCI SCIAMACHY/ENVISAT and TANSO-FTS/GOSAT CO<sub>2</sub> and CH<sub>4</sub> retrieval algorithm products with measurements from the TCCON, *Atmos. Meas. Tech.*, 7, 1723–1744, doi:10.5194/amt-7-1723-2014, 2014.
- Ebita, A., Kobayashi, S., Ota, Y., Moriya, M., Kumabe, R., Onogi, K., Harada, Y., Yasui, S., Miyaoka, K., Takahashi, K., Kama-hori, H., Kobayashi, C., Endo, H., Soma, M., Oikawa, Y., and Ishimizu, T.: The Japanese 55-year Reanalysis “JRA-55”: An interim report, *SOLA*, 7, 149–152, doi:10.2151/sola.2011-038, 2011.
- Engel, A., Möbius, T., Bönisch, H., Schmidt, U., Heinz, R., Levin, I., Atlas, E., Aoki, S., Nakazawa, T., Sugawara, S., Moore, F., Hurst, D., Elkins, J., Schauffler, S., Andrews, A., and Boering, K.: Age of stratospheric air unchanged within uncertainties over the past 30 years, *Nature Geosci.*, 2, 28–31, doi:10.1038/ngeo388, 2009.
- Fischer, H., Birk, M., Blom, C., Carli, B., Carlotti, M., von Clar-mann, T., Delbouille, L., Dudhia, A., Ehhalt, D., Endemann, M., Flaud, J. M., Gessner, R., Kleinert, A., Koopman, R., Langen, J., López-Puertas, M., Mosner, P., Nett, H., Oelhaf, H., Perron, G., Remedios, J., Ridolfi, M., Stiller, G., and Zander, R.: MIPAS: an instrument for atmospheric and climate research, *Atmos. Chem. Phys.*, 8, 2151–2188, doi:10.5194/acp-8-2151-2008, 2008.
- Frankenberg, C., Aben, I., Bergamaschi, P., Dlugokencky, E. J., van Hees, R., Houweling, S., van der Meer, P., Snel, R., and Tol, P.: Global column-averaged methane mixing ratios from 2003 to 2009 as derived from SCIAMACHY: Trends and variability, *J. Geophys. Res.*, 116, D04302, doi:10.1029/2010JD014849, 2011.
- Fraser, A., Palmer, P. I., Feng, L., Boesch, H., Cogan, A., Parker, R., Dlugokencky, E. J., Fraser, P. J., Krummel, P. B., Langenfelds, R. L., O’Doherty, S., Prinn, R. G., Steele, L. P., van der Schoot, M., and Weiss, R. F.: Estimating regional methane surface fluxes: the relative importance of surface and GOSAT mole fraction measurements, *Atmos. Chem. Phys.*, 13, 5697–5713, doi:10.5194/acp-13-5697-2013, 2013.
- Fraser, A., Palmer, P. I., Feng, L., Bösch, H., Parker, R., Dlugokencky, E. J., Krummel, P. B., and Langenfelds, R. L.: Estimating regional fluxes of CO<sub>2</sub> and CH<sub>4</sub> using space-borne observations of XCH<sub>4</sub>: XCO<sub>2</sub>, *Atmos. Chem. Phys.*, 14, 12883–12895, doi:10.5194/acp-14-12883-2014, 2014.
- Geibel, M. C., Messerschmidt, J., Gerbig, C., Blumenstock, T., Chen, H., Hase, F., Kolle, O., Lavric, J. V., Notholt, J., Palm, M., Rettinger, M., Schmidt, M., Sussmann, R., Warneke, T., and Feist, D. G.: Calibration of column-averaged CH<sub>4</sub> over European TCCON FTS sites with airborne in-situ measurements, *Atmos. Chem. Phys.*, 12, 8763–8775, doi:10.5194/acp-12-8763-2012, 2012.
- Griffith, D. W. T., Deutscher, N., Velazco, V. A., Wennberg, P. O., Yavin, Y., Keppel Aleks, G., Washenfelder, R., Toon, G. C., Blavier, J.-F., Murphy, C., Jones, N., Kettlewell, G., Connor, B., Macatangay, R., Roehl, C., Ryzek, M., Glowacki, J., Culgan, T., and Bryant, G.: TCCON data from Darwin, Australia, Release GGG2014R0, TCCON data archive, hosted by the Carbon Dioxide Information Analysis Center, Oak Ridge National Laboratory, Oak Ridge, Tennessee, USA, doi:10.14291/tcon.ggg2014.darwin01.R0/1149290, 2014a.
- Griffith, D. W. T., Velazco, V. A., Deutscher, N., Murphy, C., Jones, N., Wilson, S., Macatangay, R., Kettlewell, G., Buchholz, R. R., and Rigenbach, M.: TCCON data from Wollon-

- gong, Australia, Release GGG2014R0, TCCON data archive, hosted by the Carbon Dioxide Information Analysis Center, Oak Ridge National Laboratory, Oak Ridge, Tennessee, USA, doi:10.14291/tcon.ggg2014.wollongong01.R0/1149291, 2014b.
- Haenel, F. J., Stiller, G. P., von Clarmann, T., Funke, B., Eckert, E., Glatthor, N., Grabowski, U., Kellmann, S., Kiefer, M., Linden, A., and Reddman, T.: Reassessment of MIPAS age of air trends and variability, *Atmos. Chem. Phys.*, 15, 13161–13176, doi:10.5194/acp-15-13161-2015, 2015.
- Hase, F., Blumenstock, T., Dohe, S., Groß, J., and Kiel, M.: TCCON data from Karlsruhe, Germany, Release GGG2014R0, TCCON data archive, hosted by the Carbon Dioxide Information Analysis Center, Oak Ridge National Laboratory, Oak Ridge, Tennessee, USA, doi:10.14291/tcon.ggg2014.karlsruhe01.R0/1149270, 2014.
- Hourdin, F., Musat, I., Bony, S., Braconnot, P., Codron, F., Dufresne, J., Fairhead, L., Filiberti, M., Friedlingstein, P., Grandpeix, J., Krinner, G., Levan, P., Li, Z., and Lott, F.: The LMDz4 general circulation model: climate performance and sensitivity to parametrized physics with emphasis on tropical convection, *Clim. Dynam.*, 27, 787–813, doi:10.1007/s00382-006-0158-0, 2006.
- Houweling, S., Krol, M., Bergamaschi, P., Frankenberg, C., Dlugokencky, E. J., Morino, I., Notholt, J., Sherlock, V., Wunch, D., Beck, V., Gerbig, C., Chen, H., Kort, E. A., Röckmann, T., and Aben, I.: A multi-year methane inversion using SCIAMACHY, accounting for systematic errors using TCCON measurements, *Atmos. Chem. Phys.*, 14, 3991–4012, doi:10.5194/acp-14-3991-2014, 2014.
- Inoue, M., Morino, I., Uchino, O., Nakatsuru, T., Yoshida, Y., Yokota, T., Wunch, D., Wennberg, P. O., Roehl, C. M., Griffith, D. W. T., Velasco, V. A., Deutscher, N. M., Warneke, T., Notholt, J., Robinson, J., Sherlock, V., Hase, F., Blumenstock, T., Rettinger, M., Sussmann, R., Kyrö, E., Kivi, R., Shiomi, K., Kawakami, S., De Mazière, M., Arnold, S. G., Feist, D. G., Barrow, E. A., Barney, J., Dubey, M., Schneider, M., Iraci, L. T., Podolske, J. R., Hillyard, P. W., Machida, T., Sawa, Y., Tsuboi, K., Matsueda, H., Sweeney, C., Tans, P. P., Andrews, A. E., Biraud, S. C., Fukuyama, Y., Pittman, J. V., Kort, E. A., and Tanaka, T.: Bias corrections of GOSAT SWIR XCO<sub>2</sub> and XCH<sub>4</sub> with TCCON data and their evaluation using aircraft measurement data, *Atmos. Meas. Tech.*, 9, 3491–3512, doi:10.5194/amt-9-3491-2016, 2016.
- Karion, A., Sweeney, C., Tans, P., and Newberger, T.: Aircore: an innovative atmospheric sampling system, *J. Atmos. Ocean. Tech.*, 27, 1839–1853, doi:10.1175/2010JTECHA1448.1, 2010.
- Kivi, R., Heikkinen, P., and Kyro, E.: TCCON data from Sodankylä, Finland, Release GGG2014R0, TCCON data archive, hosted by the Carbon Dioxide Information Analysis Center, Oak Ridge National Laboratory, Oak Ridge, Tennessee, USA, doi:10.14291/tcon.ggg2014.sodankyla01.R0/1149280, 2014.
- Krol, M., Houweling, S., Bregman, B., van den Broek, M., Segers, A., van Velthoven, P., Peters, W., Dentener, F., and Bergamaschi, P.: The two-way nested global chemistry-transport zoom model TM5: algorithm and applications, *Atmos. Chem. Phys.*, 5, 417–432, doi:10.5194/acp-5-417-2005, 2005.
- Kulawik, S., Wunch, D., O'Dell, C., Frankenberg, C., Reuter, M., Oda, T., Chevallier, F., Sherlock, V., Buchwitz, M., Osterman, G., Miller, C. E., Wennberg, P. O., Griffith, D., Morino, I., Dubey, M. K., Deutscher, N. M., Notholt, J., Hase, F., Warneke, T., Sussmann, R., Robinson, J., Strong, K., Schneider, M., De Mazière, M., Shiomi, K., Feist, D. G., Iraci, L. T., and Wolf, J.: Consistent evaluation of ACOS-GOSAT, BESD-SCIAMACHY, CarbonTracker, and MACC through comparisons to TCCON, *Atmos. Meas. Tech.*, 9, 683–709, doi:10.5194/amt-9-683-2016, 2016.
- Kurylo, M. J.: Network for the detection of stratospheric change, *Proc. SPIE*, 1491, 168–174, doi:10.1117/12.46658, 1991.
- Kuze, A., Suto, H., Nakajima, M., and Hamazaki, T.: Thermal and near infrared sensor for carbon observation Fourier-transform spectrometer on the Greenhouse Gases Observing SATellite for greenhouse gases monitoring, *Appl. Opt.*, 48, 6716–6733, doi:10.1364/AO.48.006716, 2009.
- Laeng, A., Plieninger, J., von Clarmann, T., Grabowski, U., Stiller, G., Eckert, E., Glatthor, N., Haenel, F., Kellmann, S., Kiefer, M., Linden, A., Lossow, S., Deaver, L., Engel, A., Hervig, M., Levin, I., McHugh, M., Noël, S., Toon, G., and Walker, K.: Validation of MIPAS IMK/IAA methane profiles, *Atmos. Meas. Tech.*, 8, 5251–5261, doi:10.5194/amt-8-5251-2015, 2015.
- Locatelli, R., Bousquet, P., Chevallier, F., Fortems-Cheney, A., Szopa, S., Saunio, M., Agustí-Panareda, A., Bergmann, D., Bian, H., Cameron-Smith, P., Chipperfield, M. P., Gloor, E., Houweling, S., Kawa, S. R., Krol, M., Patra, P. K., Prinn, R. G., Rigby, M., Saito, R., and Wilson, C.: Impact of transport model errors on the global and regional methane emissions estimated by inverse modelling, *Atmos. Chem. Phys.*, 13, 9917–9937, doi:10.5194/acp-13-9917-2013, 2013.
- Locatelli, R., Bousquet, P., Saunio, M., Chevallier, F., and Cressot, C.: Sensitivity of the recent methane budget to LMDz sub-grid-scale physical parameterizations, *Atmos. Chem. Phys.*, 15, 9765–9780, doi:10.5194/acp-15-9765-2015, 2015.
- Meirink, J. F., Bergamaschi, P., and Krol, M. C.: Four-dimensional variational data assimilation for inverse modelling of atmospheric methane emissions: method and comparison with synthesis inversion, *Atmos. Chem. Phys.*, 8, 6341–6353, doi:10.5194/acp-8-6341-2008, 2008.
- Messerschmidt, J., Geibel, M. C., Blumenstock, T., Chen, H., Deutscher, N. M., Engel, A., Feist, D. G., Gerbig, C., Gisi, M., Hase, F., Katrynski, K., Kolle, O., Lavric, J. V., Notholt, J., Palm, M., Ramonet, M., Rettinger, M., Schmidt, M., Sussmann, R., Toon, G. C., Truong, F., Warneke, T., Wennberg, P. O., Wunch, D., and Xueref-Remy, I.: Calibration of TCCON column-averaged CO<sub>2</sub>: the first aircraft campaign over European TCCON sites, *Atmos. Chem. Phys.*, 11, 10765–10777, doi:10.5194/acp-11-10765-2011, 2011.
- Monge-Sanz, B. M., Chipperfield, M. P., Simmons, A. J., and Uppala, S. M.: Mean age of air and transport in a CTM: comparison of different ECMWF analyses, *Geophys. Res. Lett.*, 340, L04801, doi:10.1029/2006GL028515, 2007.
- Monge-Sanz, B. M., Chipperfield, M. P., Dee, D. P., Simmons, A. J., and Uppala, S. M.: Improvements in the stratospheric transport achieved by a chemistry transport model with ECMWF (re)analyses: identifying effects and remaining challenges, *Q. J. Roy. Meteor. Soc.*, 139, 654–673, doi:10.1002/qj.1996, 2013.
- Monteil, G., Houweling, S., Butz, A., Guerlet, S., Schepers, D., Hasekamp, O., Frankenberg, C., Scheepmaker, R., Aben, I., and Röckmann, T.: Comparison of CH<sub>4</sub> inversions based on 15

- months of GOSAT and SCIAMACHY observations, *J. Geophys. Res.-Atmos.*, 118, 11807–11823, doi:10.1002/2013JD019760, 2013.
- Onogi, K., Tsutusi, J., Koide, H., Sakamoto, M., Kobayashi, S., Hat-sushika, H., Matsumoto, T., Yamazaki, N., Kamahori, H., Takahashi, K., Kadokura, S., Wada, K., Kato, K., Oyama, R., Ose, T., Mannoji, N., and Taira, R.: The JRA-25 reanalysis, *J. Meteorol. Soc. Jpn.*, 85, 369–432, 2007.
- Ostler, A., Sussmann, R., Rettinger, M., Deutscher, N. M., Dohe, S., Hase, F., Jones, N., Palm, M., and Sinnhuber, B.-M.: Multistation intercomparison of column-averaged methane from NDACC and TCCON: impact of dynamical variability, *Atmos. Meas. Tech.*, 7, 4081–4101, doi:10.5194/amt-7-4081-2014, 2014.
- Pandey, S., Houweling, S., Krol, M., Aben, I., Chevallier, F., Dlugokencky, E. J., Gatti, L. V., Gloor, E., Miller, J. B., Detmers, R., Machida, T., and Röckmann, T.: Inverse modeling of GOSAT-retrieved ratios of total column CH<sub>4</sub> and CO<sub>2</sub> for 2009 and 2010, *Atmos. Chem. Phys.*, 16, 5043–5062, doi:10.5194/acp-16-5043-2016, 2016.
- Parker, R., Boesch, H., Cogan, A., Fraser, A., Feng, L., Palmer, P. I., Messerschmidt, J., Deutscher, N., Griffith, D. W. T., Notholt, J., Wennberg, P. O., and Wunch, D.: Methane observations from the Greenhouse Gases Observing SATellite: Comparison to ground-based TCCON data and model calculations, *Geophys. Res. Lett.*, 38, L15807, doi:10.1029/2011GL047871, 2011.
- Parker, R. J., Boesch, H., Byckling, K., Webb, A. J., Palmer, P. I., Feng, L., Bergamaschi, P., Chevallier, F., Notholt, J., Deutscher, N., Warneke, T., Hase, F., Sussmann, R., Kawakami, S., Kivi, R., Griffith, D. W. T., and Velazco, V.: Assessing 5 years of GOSAT Proxy XCH<sub>4</sub> data and associated uncertainties, *Atmos. Meas. Tech.*, 8, 4785–4801, doi:10.5194/amt-8-4785-2015, 2015.
- Patra, P. K., Takigawa, M., Ishijima, K., Choi, B.-C., Cunnold, D., Dlugokencky, E. J., Fraser, P., Gomez-Pelaez, A. J., Goo, T.-Y., Kim, J.-S., Krummel, P., Langenfelds, R., Meinhardt, F., Mukai, H., O'Doherty, S., Prinn, R. G., Simmonds, P., Steele, P., Tohjima, Y., Tsuboi, K., Uhse, K., Weiss, R., Worthy, D., and Nakazawa, T.: Growth rate, seasonal, synoptic, diurnal variations and budget of methane in lower atmosphere, *J. Meteorol. Soc. Jpn.*, 87, 635–663, 2009a.
- Patra, P. K., Takigawa, M., Dutton, G. S., Uhse, K., Ishijima, K., Lintner, B. R., Miyazaki, K., and Elkins, J. W.: Transport mechanisms for synoptic, seasonal and interannual SF<sub>6</sub> variations and “age” of air in troposphere, *Atmos. Chem. Phys.*, 9, 1209–1225, doi:10.5194/acp-9-1209-2009, 2009b.
- Patra, P. K., Houweling, S., Krol, M., Bousquet, P., Belikov, D., Bergmann, D., Bian, H., Cameron-Smith, P., Chipperfield, M. P., Corbin, K., Fortems-Cheiney, A., Fraser, A., Gloor, E., Hess, P., Ito, A., Kawa, S. R., Law, R. M., Loh, Z., Maksyutov, S., Meng, L., Palmer, P. I., Prinn, R. G., Rigby, M., Saito, R., and Wilson, C.: TransCom model simulations of CH<sub>4</sub> and related species: linking transport, surface flux and chemical loss with CH<sub>4</sub> variability in the troposphere and lower stratosphere, *Atmos. Chem. Phys.*, 11, 12813–12837, doi:10.5194/acp-11-12813-2011, 2011.
- Patra, P. K., Krol, M. C., Montzka, S. A., Arnold, T., Atlas, E. L., Lintner, B. R., Stephens, B. B., Xiang, B., Elkins, J. W., Fraser, P. J., Ghosh, A., Hints, E. J., Hurst, D. F., Ishijima, K., Krummel, P. B., Miller, B. R., Miyazaki, K., Moore, F. L., Mühle, J., O'Doherty, S., Prinn, R. G., Steele, L. P., Takigawa, M., Wang, H. J., Weiss, R. F., Wofsy, S. C., and Young, D.: Observational evidence for interhemispheric hydroxyl parity, *Nature*, 513, 219–223, doi:10.1038/nature13721, 2014.
- Patra, P. K., Saeki, T., Dlugokencky, E. J., Ishijima, K., Umezawa, T., Ito, A., Aoki, S., Morimoto, S., Kort, E. A., Crotwell, A., Ravi Kumar, K., and Nakazawa, T.: Regional methane emission estimation based on observed atmospheric concentrations (2002–2012), *J. Meteorol. Soc. Jpn.*, 94, 91–113, doi:10.2151/jmsj.2016-006, 2016.
- Pliening, J., von Clarmann, T., Stiller, G. P., Grabowski, U., Glatthor, N., Kellmann, S., Linden, A., Haenel, F., Kiefer, M., Höpfner, M., Laeng, A., and Lossow, S.: Methane and nitrous oxide retrievals from MIPAS-ENVISAT, *Atmos. Meas. Tech.*, 8, 4657–4670, doi:10.5194/amt-8-4657-2015, 2015.
- Pliening, J., Laeng, A., Lossow, S., von Clarmann, T., Stiller, G. P., Kellmann, S., Linden, A., Kiefer, M., Walker, K. A., Noël, S., Hervig, M. E., McHugh, M., Lambert, A., Urban, J., Elkins, J. W., and Murtagh, D.: Validation of revised methane and nitrous oxide profiles from MIPAS-ENVISAT, *Atmos. Meas. Tech.*, 9, 765–779, doi:10.5194/amt-9-765-2016, 2016.
- Saad, K. M., Wunch, D., Toon, G. C., Bernath, P., Boone, C., Connor, B., Deutscher, N. M., Griffith, D. W. T., Kivi, R., Notholt, J., Roehl, C., Schneider, M., Sherlock, V., and Wennberg, P. O.: Derivation of tropospheric methane from TCCON CH<sub>4</sub> and HF total column observations, *Atmos. Meas. Tech.*, 7, 2907–2918, doi:10.5194/amt-7-2907-2014, 2014.
- Saito, R., Patra, P. K., Deutscher, N., Wunch, D., Ishijima, K., Sherlock, V., Blumenstock, T., Dohe, S., Griffith, D., Hase, F., Heikkinen, P., Kyrö, E., Macatangay, R., Mendonca, J., Messerschmidt, J., Morino, I., Notholt, J., Rettinger, M., Strong, K., Sussmann, R., and Warneke, T.: Technical Note: Latitude-time variations of atmospheric column-average dry air mole fractions of CO<sub>2</sub>, CH<sub>4</sub> and N<sub>2</sub>O, *Atmos. Chem. Phys.*, 12, 7767–7777, doi:10.5194/acp-12-7767-2012, 2012.
- Schepers, D., Guerlet, S., Butz, A., Landgraf, J., Frankenberg, C., Hasekamp, O., Blavier, J.-F., Deutscher, N. M., Griffith, D. W. T., Hase, F., Kyro, E., Morino, I., Sherlock, V., Sussmann, R., and Aben, I.: Methane retrievals from Greenhouse Gases Observing Satellite (GOSAT) shortwave infrared measurements: Performance comparison of proxy and physics retrieval algorithms, *J. Geophys. Res.*, 117, D10307, doi:10.1029/2012JD017549, 2012.
- Sepúlveda, E., Schneider, M., Hase, F., García, O. E., Gomez-Pelaez, A., Dohe, S., Blumenstock, T., and Guerra, J. C.: Long-term validation of tropospheric column-averaged CH<sub>4</sub> mole fractions obtained by mid-infrared ground-based FTIR spectrometry, *Atmos. Meas. Tech.*, 5, 1425–1441, doi:10.5194/amt-5-1425-2012, 2012.
- Sepúlveda, E., Schneider, M., Hase, F., Barthlott, S., Dubravica, D., García, O. E., Gomez-Pelaez, A., González, Y., Guerra, J. C., Gisi, M., Kohlhepp, R., Dohe, S., Blumenstock, T., Strong, K., Weaver, D., Palm, M., Sadeghi, A., Deutscher, N. M., Warneke, T., Notholt, J., Jones, N., Griffith, D. W. T., Smale, D., Brailsford, G. W., Robinson, J., Meinhardt, F., Steinbacher, M., Aalto, T., and Worthy, D.: Tropospheric CH<sub>4</sub> signals as observed by NDACC FTIR at globally distributed sites and comparison to GAW surface in situ measurements, *Atmos. Meas. Tech.*, 7, 2337–2360, doi:10.5194/amt-7-2337-2014, 2014.
- Sherlock, V., Connor, B., Robinson, J., Shiona, H., Smale, D., and Pollard, D.: TCCON data from Lauder, New Zealand, 120HR, Release GGG2014R0, TCCON data archive, hosted

- by the Carbon Dioxide Information Analysis Center, Oak Ridge National Laboratory, Oak Ridge, Tennessee, USA, doi:10.14291/tcon.ggg2014.lauder01.R0/1149293, 2014a.
- Sherlock, V., B., Connor, B., Robinson, J., Shiona, H., Smale, D., and Pollard, D.: TCCON data from Lauder, New Zealand, 125HR, Release GGG2014R0, TCCON data archive, hosted by the Carbon Dioxide Information Analysis Center, Oak Ridge National Laboratory, Oak Ridge, Tennessee, USA, doi:10.14291/tcon.ggg2014.lauder02.R0/1149298, 2014b.
- Spivakovsky, C. M., Logan, J. A., Montzka, S. A., Balkanski, Y. J., Foreman-Fowler, M., Jones, D. B. A., Horowitz, L. W., Fusco, A. C., Brenninkmeijer, C. A. M., Prather, M. J., Wofsy, S. C., and McElroy, M. B.: Three-dimensional climatological distribution of tropospheric OH: Update and evaluation, *J. Geophys. Res.*, 105, 8931–8980, doi:10.1029/1999JD901006, 2000.
- Stiller, G. P., von Clarmann, T., Haenel, F., Funke, B., Glatthor, N., Grabowski, U., Kellmann, S., Kiefer, M., Linden, A., Losow, S., and López-Puertas, M.: Observed temporal evolution of global mean age of stratospheric air for the 2002 to 2010 period, *Atmos. Chem. Phys.*, 12, 3311–3331, doi:10.5194/acp-12-3311-2012, 2012.
- Strahan, S., Douglass, A., Stolarski, E., Akiyoshi, H., Bekki, S., Braesicke, P., Butchart, N., Chipperfield, M. P., Cugnet, D., Dhomse, S., Frith, S. M., Gettelman, A., Hardiman, S. C., Kinnison, D. E., Lamarque, J. F., Mancini, E., Marchand, M., Michou, M., Morgenstern, O., Nakamura, T., Olivie, D., Pawson, S., Pitari, G., Plummer, D. A., Pyle, J. A., Scinocca, J. F., Shepherd, T. G., Shibata, K., Smale, D., Teyssedre, H., Tian, W., and Yamashita, Y.: Using transport diagnostics to understand chemistry climate model ozone simulations, *J. Geophys. Res.*, 116, D17302, doi:10.1029/2010JD015360, 2011.
- Sussmann, R. and Rettinger, M.: TCCON data from Garmisch, Germany, Release GGG2014R0. TCCON data archive, hosted by the Carbon Dioxide Information Analysis Center, Oak Ridge National Laboratory, Oak Ridge, Tennessee, USA, doi:10.14291/tcon.ggg2014.garmisch01.R0/1149299, 2014.
- Sussmann, R., Forster, F., Rettinger, M., and Jones, N.: Strategy for high-accuracy-and-precision retrieval of atmospheric methane from the mid-infrared FTIR network, *Atmos. Meas. Tech.*, 4, 1943–1964, doi:10.5194/amt-4-1943-2011, 2011.
- Sussmann, R., Forster, F., Rettinger, M., and Bousquet, P.: Renewed methane increase for five years (2007–2011) observed by solar FTIR spectrometry, *Atmos. Chem. Phys.*, 12, 4885–4891, doi:10.5194/acp-12-4885-2012, 2012.
- Sussmann, R., Ostler, A., Forster, F., Rettinger, M., Deutscher, N. M., Griffith, D. W. T., Hannigan, J. W., Jones, N., and Patra, P. K.: First intercalibration of column-averaged methane from the Total Carbon Column Observing Network and the Network for the Detection of Atmospheric Composition Change, *Atmos. Meas. Tech.*, 6, 397–418, doi:10.5194/amt-6-397-2013, 2013.
- Szopa, S., Balkanski, Y., Schulz, M., Bekki, S., Cugnet, D., Fortems-Cheiney, A., Turquety, S., Cozic, A., Déandréis, C., Hauglustaine, D., Idelkadi, A., Lathière, J., Lefevre, F., Marchand, M., Vuolo, R., Yan, N., and Dufresne, J.-L.: Aerosol and ozone changes as forcing for climate evolution between 1850 and 2100, *Clim. Dynam.*, 40, 2223–2250, doi:10.1007/s00382-012-1408-y, 2013.
- Takigawa, M., Takahashi, M., and Akiyoshi, H.: Simulation of ozone and other chemical species using a Center for Climate System Research/National Institute for Environmental Studies atmospheric GCM with coupled stratospheric chemistry, *J. Geophys. Res.*, 104, 14003–14018, doi:10.1029/1998JD100105, 1999.
- Turner, A. J., Jacob, D. J., Wecht, K. J., Maasackers, J. D., Lundgren, E., Andrews, A. E., Biraud, S. C., Boesch, H., Bowman, K. W., Deutscher, N. M., Dubey, M. K., Griffith, D. W. T., Hase, F., Kuze, A., Notholt, J., Ohyama, H., Parker, R., Payne, V. H., Sussmann, R., Sweeney, C., Velasco, V. A., Warneke, T., Wennberg, P. O., and Wunch, D.: Estimating global and North American methane emissions with high spatial resolution using GOSAT satellite data, *Atmos. Chem. Phys.*, 15, 7049–7069, doi:10.5194/acp-15-7049-2015, 2015.
- von Clarmann, T., Glatthor, N., Grabowski, U., Höpfner, M., Kellmann, S., Kiefer, M., Linden, A., Mengistu Tsidu, G., Milz, M., Steck, T., Stiller, G. P., Wang, D.-Y., Fischer, H., Funke, B., Gil-López, S., and López-Puertas, M.: Retrieval of temperature and tangent altitude pointing from limb emission spectra recorded from space by the Michelson Interferometer for Passive Atmospheric Sounding (MIPAS), *J. Geophys. Res.*, 108, 4736, doi:10.1029/2003JD003602, 2003.
- Wang, Z., Deutscher, N. M., Warneke, T., Notholt, J., Dils, B., Griffith, D. W. T., Schmidt, M., Ramonet, M., and Gerbig, C.: Retrieval of tropospheric column-averaged CH<sub>4</sub> mole fraction by solar absorption FTIR-spectrometry using N<sub>2</sub>O as a proxy, *Atmos. Meas. Tech.*, 7, 3295–3305, doi:10.5194/amt-7-3295-2014, 2014.
- Warneke, T., Messerschmidt, J., Notholt, J., Weinzierl, C., Deutscher, N., Petri, C., Gruppe, P., Vuillemin, C., Truong, F., Schmidt, M., Ramonet, M., and Parmentier, E.: TCCON data from Orleans, France, Release GGG2014R0, TCCON data archive, hosted by the Carbon Dioxide Information Analysis Center, Oak Ridge National Laboratory, Oak Ridge, Tennessee, USA, doi:10.14291/tcon.ggg2014.orleans01.R0/1149276, 2014.
- Washenfelder, R. A., Wennberg, P. O., and Toon, G. C.: Tropospheric methane retrieved from ground-based near-IR solar absorption spectra, *Geophys. Res. Lett.*, 30, 2226, doi:10.1029/2003GL017969, 2003.
- Waugh, D. W. and Hall T. M.: Age of stratospheric air: Theory, observations, and models, *Rev. Geophys.*, 40, 1010, doi:10.1029/2000RG000101, 2002.
- Wecht, K. J., Jacob D. J., Frankenberg C., Jiang Z., and Blake D. R.: Mapping of North American methane emissions with high spatial resolution by inversion of SCIAMACHY satellite data, *J. Geophys. Res.-Atmos.*, 119, 7741–7756, doi:10.1002/2014JD021551, 2014.
- Wennberg, P. O., Wunch, D., Roehl, C., Blavier, J.-F., Toon, G. C., Allen, N., Dowell, P., Teske, K., Martin, C., and Martin, J.: TCCON data from Lamont, Oklahoma, USA, Release GGG2014R0. TCCON data archive, hosted by the Carbon Dioxide Information Analysis Center, Oak Ridge National Laboratory, Oak Ridge, Tennessee, USA, doi:10.14291/tcon.ggg2014.lamont01.R0/1149159, 2014a.
- Wennberg, P. O., Roehl, C., Wunch, D., Toon, G. C., Blavier, J.-F., Washenfelder, R., Keppel-Aleks, G., Allen, N., and Ayers, J.: TCCON data from Park Falls, Wisconsin, USA, Release GGG2014R0, TCCON data archive, hosted by the Carbon Dioxide Information Analysis Center, Oak



- Ridge National Laboratory, Oak Ridge, Tennessee, USA, doi:10.14291/tccon.ggg2014.parkfalls01.R0/1149161, 2014b.
- Wunch, D., Toon, G. C., Wennberg, P. O., Wofsy, S. C., Stephens, B. B., Fischer, M. L., Uchino, O., Abshire, J. B., Bernath, P., Biraud, S. C., Blavier, J.-F. L., Boone, C., Bowman, K. P., Browell, E. V., Campos, T., Connor, B. J., Daube, B. C., Deutscher, N. M., Diao, M., Elkins, J. W., Gerbig, C., Gottlieb, E., Griffith, D. W. T., Hurst, D. F., Jiménez, R., Keppel-Aleks, G., Kort, E. A., Macatangay, R., Machida, T., Matsueda, H., Moore, F., Morino, I., Park, S., Robinson, J., Roehl, C. M., Sawa, Y., Sherlock, V., Sweeney, C., Tanaka, T., and Zondlo, M. A.: Calibration of the Total Carbon Column Observing Network using aircraft profile data, *Atmos. Meas. Tech.*, 3, 1351–1362, doi:10.5194/amt-3-1351-2010, 2010.
- Wunch, D., Toon, G. C., Blavier, J.-F. L., Washenfelder, R. A., Notholt, J., Connor, B. J., Griffith, D. W. T., Sherlock, V., and Wennberg, P. O.: The Total Carbon Column Observing Network, *Phil. Trans. R. Soc. A*, 369, 2087–2112, doi:10.1098/rsta.2010.0240, 2011.
- Yokota, T., Yoshida, Y., Eguchi, N., Ota, Y., Tanaka, T., Watanabe, H., and Maksyutov, S.: Global concentrations of CO<sub>2</sub> and CH<sub>4</sub> retrieved from GOSAT, first preliminary results, *SOLA*, 5, 160–163, doi:10.2151/sola.2009-041, 2009.